Leggett-Garg tests of macrorealism for bosonic systems including double-well Bose-Einstein condensates and atom interferometers

L. Rosales-Zárate,[1,2] B. Opanchuk,[1] Q. Y. He,[3] and M. D. Reid[1]
[1]*Centre for Quantum and Optical Science, Swinburne University of Technology, Melbourne 3122, Australia*
[2]*Centro de Investigaciones en Óptica A.C., León, Guanajuato 37150, Mexico*
[3]*State Key Laboratory of Mesoscopic Physics, School of Physics, Peking University, Beijing 100871, China*

(Received 15 December 2016; revised manuscript received 16 December 2017; published 19 April 2018)

We construct quantifiable generalizations of Leggett-Garg tests for macro- and mesoscopic realism and noninvasive measurability that apply when not all outcomes of measurement can be identified as arising from one of two macroscopically distinguishable states. We show how quantum mechanics predicts a negation of the Leggett-Garg premises for strategies involving ideal negative-result, weak, and minimally invasive ("nonclumsy") projective measurements on dynamical entangled systems, as might be realized with Bose-Einstein condensates in a double-well potential, path-entangled NOON states, and atom interferometers. Potential loopholes associated with each strategy are discussed.

DOI: 10.1103/PhysRevA.97.042114

I. INTRODUCTION

In his paradox where a cat is apparently both dead and alive, Schrödinger raised the possibility of an inconsistency between macroscopic realism and quantum mechanics [1]. Leggett-Garg suggested testing macroscopic realism by comparing the predictions of quantum mechanics with those based on two classical premises [2]. The first premise is *macroscopic realism per se* (MR or MRPS): a macroscopic system with two macroscopically distinguishable states available to it will at all times be in one or other of these states. The second premise is *macroscopic noninvasive measurability* (NIM): for such a system, it is possible, in principle, to determine which of these states the system is in, with arbitrarily small perturbation on the subsequent dynamics.

Leggett and Garg showed how the two premises (referred to as macrorealism) constrain the dynamics of a two-state system. Considering three successive times $t_3 > t_2 > t_1$, the variable S_i denotes which of the two states the system is in at time t_i, the respective states being denoted by $S_i = +1$ or -1. The Leggett-Garg premises imply the Leggett-Garg inequality [2,3]

$$LG \equiv \langle S_1 S_2\rangle + \langle S_2 S_3\rangle - \langle S_1 S_3\rangle \leqslant 1. \tag{1}$$

More recent work shows how the Leggett-Garg premises also imply the "no disturbance" or "no signaling in time" condition [4,5]

$$d_\sigma \equiv \langle S_3|\hat{M}_2,\sigma\rangle - \langle S_3|\sigma\rangle = 0. \tag{2}$$

Here $\langle S_3|\hat{M}_2,\sigma\rangle$ (and $\langle S_3|\sigma\rangle$) is the expectation value of S_3 given that a measurement $\hat{M}_2$ is performed (or not performed) at time t_2, conditional on the system being prepared in a state denoted by σ at time t_1. The Leggett-Garg inequality and no-disturbance conditions are predicted to be violated for many quantum systems where the dynamics involves the formation of quantum superposition states [2–17]. The work of Leggett and Garg represented an advance, since it extended beyond the quantum framework to show how the macroscopic quantum superposition state defies classical macroscopic reality.

The Leggett-Garg approach raised new ideas about how to test quantum mechanics even at the microscopic level [5,6,8–11]. Failure of the inequalities implies no classical trajectory exists between successive measurements: either the system cannot be viewed as being in a definite state independent of observation, or there cannot be a way to determine that state, without interference by the measurement. Noninvasive measurability is "vexing" to justify, however, because of the plausibility of the measurement disturbing the system. Leggett and Garg countered this problem by proposing an ideal negative-result (INR) measurement: the argument is conditional on the first postulate being true, e.g., *if* a photon does travel through one slit *or* the other, a null detection beyond one slit is justified to be noninvasive [2,9,10,14]. A second approach is to perform weak measurements [18–21] enabling calculation of the moment $\langle S_2 S_3\rangle$ in a limit where there is a vanishing disturbance to the system [11–13,20,22]. A third approach is to justify certain projective measurements as being minimally invasive, or "nonclumsy (NC)", if indeed the system is in one state or the other. Related methods test modified Leggett-Garg inequalities that quantify the invasiveness of "clumsy" projective and/or quantum nondemolition (QND) measurements [4,17,23]. So far, experimental investigations have mainly focused on superconducting circuits or small systems (e.g., single atoms or photons). Recent developments include theoretical proposals for mechanical oscillators [16] and macroscopic states of atoms [17].

An illuminating Leggett-Garg test would involve a mesoscopic or macroscopic massive system in a quantum superposition of two states with different centre-of-mass locations [24]. In fact, as of yet, there has to our knowledge been no Leggett-Garg test involving a mesoscopic system (of several atoms or photons, or more) that is at time t_2 in a quantum superposition of spatially separated states. An example of such a superposition is the path-entangled NOON state, written as $|\psi\rangle = \frac{1}{\sqrt{2}}\{|N\rangle_a|0\rangle_b + |0\rangle_a|N\rangle_b\}$ where $|N\rangle_{a/b}$ is the

N-particle state for two spatially separated modes denoted by a and b [25–27]. In this case the ideal negative-result measurement can be applied and justified as noninvasive by the assumption of Bell's locality [28]. For massive systems, this is especially interesting [24]. The NIM premise is then based on the assumptions that the system must be located either "here" or "there," and that there is no disturbance to a massive system due to a measurement performed on a vacuum at a different location.

In this paper, we show how such tests may be possible on a mesoscopic scale. As one example, in Secs. II and III, we show that violations of Leggett-Garg inequalities are predicted for weakly linked Bose-Einstein condensates (BECs) trapped in two separated potential wells of an optical lattice. Here dynamical oscillation of large groups of atoms to form macroscopic superposition states is predicted possible for sufficient nonlinearity [29–35]. We also note that, to date, there has been no Leggett-Garg test based on matter-wave interference with BECs, despite that these systems exhibit entanglement [36–43], have demonstrated Josephson oscillation [29], and are likely candidates for mesoscopic superpositions of states with a distinct center of mass [31].

A problem, however, for an experimental realization is the fragility of the macroscopic superpositions. Under specific conditions, NOON states can be generated, allowing an ideal negative-result strategy. Otherwise, for less fragile macroscopic superposition states, we derive in Sec. IV *modified s-scopic Leggett-Garg inequalities* that can be used to test Leggett-Garg premises for superpositions of the type $|\psi\rangle = \frac{1}{\sqrt{2}}\{|N-n\rangle_a|n\rangle_b + |n\rangle_a|N-n\rangle_b\}$ ($n < N$). These superpositions deviate from the ideal NOON superposition by allowing mode population differences not equal to $-N$ or N. The modified Leggett-Garg inequalities are thus useful where outcomes are not always constrained to being "dead" or "alive" and allow a quantification of the degree of realism that is being tested. In the proposals of this paper, the relevant measure of macroscopicity is the mass difference given by sm_A (in each mode) of the two states forming the superposition, m_A being the mass of each atom.

The ideal negative-result strategy may be difficult to apply where there are residual atoms in both modes, or where spatial separation at time t_2 is not possible. We thus develop (in Secs. III B and III C) strong and weak measurement strategies for testing the Leggett-Garg premises in these cases. This opens the way to violate Leggett-Garg inequalities and to demonstrate mesoscopic quantum coherence in experiments of the type performed by Albiez *et al.* [29]. Albiez *et al.* observed oscillation of the relative populations of two weakly linked BECs across the two wells of a double-well potential created in an optical lattice and separated by $\sim 5\ \mu$m.

The strategies and inequalities developed in this paper are applicable to atomic and photonic interferometers involving multiparticle bosonic states. In Sec. IV we show how to test the Leggett-Garg premises where mesoscopic states are created at the time t_2 within the interferometer, and a subsequent measurement is made at time t_3 of the population difference after passage through the interferometer. This approach can be applied to either nonlinear interferometers where the bosons are subject to nonlinearity due to a medium, or to linear interferometers that use only beam splitters, conditional measurements, and phase shifts. In this context, we discuss violations of the s-scopic Leggett-Garg inequalities in which the two premises of MRPS and NIM are asymmetrically quantified, being specified by two different parameters s_2 and s_3.

For linear interferometers, while violation of mesoscopic Leggett-Garg inequalities may be difficult, it is nonetheless possible in principle to test the Leggett-Garg premises as applied to individual particle trajectories. This provides an avenue for a Leggett-Garg test using matter waves passing through an interferometer, that would demonstrate the "no classical trajectories" result for atoms. By exploiting different spatial separations and atomic species, such tests would enhance the experimental tests of Robens *et al.*, which showed violation of a Leggett-Garg inequality for a cesium atom performing a quantum walk [10]. In that case, the spread in distance of the atomic wave function was reported to be $\sim 2\ \mu$m.

To conclude, in Sec. V we give a discussion of loopholes for each of the strategies presented in this paper, as seen from the perspective of a macrorealist committed to the premises of Leggett and Garg. Loopholes arise from the need to make a measurement at the time t_2 in order to evaluate the two-time correlation function $\langle S_2 S_3\rangle$ correctly. For each of the three strategies, there are additional assumptions justifying that the measurement employed in the experiment will give the same correlation function for the Leggett-Garg inequality as the noninvasive measurement defined by the NIM Leggett-Garg premise. These additional assumptions imply that for each strategy, a somewhat different model for macrorealism is tested.

II. QUANTUM DYNAMICS OF A MESOSCOPIC TWO-STATE OSCILLATION

The Hamiltonian H_I for an N-atom condensate constrained to a double-well potential reveals a regime of macroscopic two-state dynamics. The two-well system has been reliably modeled by the two-mode Josephson Hamiltonian [29–39,41–44]:

$$H_I = 2\kappa \hat{J}_x + g\hat{J}_z^2. \qquad (3)$$

Here $\hat{J}_z = (\hat{a}^\dagger\hat{a} - \hat{b}^\dagger\hat{b})/2$, $\hat{J}_x = (\hat{a}^\dagger\hat{b} + \hat{b}^\dagger\hat{a})/2$, $\hat{J}_y = (\hat{a}^\dagger\hat{b} - \hat{b}^\dagger\hat{a})/2i$ are the Schwinger spin operators defined in terms of the boson operators $\hat{a}^\dagger$,$\hat{a}$ and $\hat{b}^\dagger$,$\hat{b}$, for the modes describing particles in each of the wells, labeled a and b, respectively. The κ represents interwell hopping and g the nonlinear self-interaction due to the medium. For high interaction strength ($Ng/\kappa \gg 1$), regimes exist where a mesoscopic two-state oscillation (of period T_N) takes place (Fig. 1) [30,31,33]. For such regimes, if the system is prepared in $|N\rangle_a|0\rangle_b$, then at a later time t' the state vector is to a good approximation (apart from a phase factor)

$$|\psi(t)\rangle = \cos(t)|N\rangle|0\rangle + i\sin(t)|0\rangle|N\rangle, \qquad (4)$$

where $t = E_\Delta t'/\hbar$ and E_Δ is the energy splitting of the energy eigenstates $|N\rangle|0\rangle \pm |0\rangle|N\rangle$ under H_I. In one state, $|N\rangle_a|0\rangle_b$, all N atoms are in the well a, and in the second state, $|0\rangle_a|N\rangle_b$, all atoms are in the well b [33]. The interaction H_I also describes Josephson effects in superconductors [45], superfluids [46], and exciton polaritons [47].

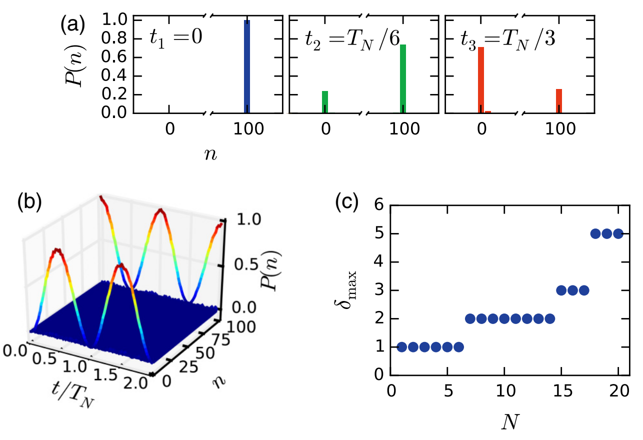

FIG. 1. Two-state NOON dynamics: (a) The probability $P(n)$ of n atoms in well a at times 0, $T_N/6$, $T_N/3$. Here $N = 100$, $g/\kappa = 1$. T_N is the two-state oscillation period. The system undergoes oscillation between two states, where all atoms are in one or other well. The probability of obtaining results other than $n = 0$ or 100 is negligible. The Leggett-Garg inequality (1) is violated with $LG = 1.5$ for states distinct by $s = 100$ atoms in each well. (b) $P(n)$ versus time t for the system described in (a). (c) An upper bound on the backaction δ due to the ideal negative-result (INR) measurement that can be tolerated for an Leggett-Garg violation. Here δ is plotted versus N, the total number of atoms in the system.

The quantum solution (4) predicts a violation of the Leggett-Garg inequality [34]. Here we denote the sign of the outcome J_z of the spin measurement $\hat{J}_z$ at time t_i by S_i ($S_i = 1$ if $J_z \geqslant 0$; $S_i = -1$ if $J_z < 0$). The associated quantum measurement is denoted $\hat{S}_i$. The two-time correlation $\langle S_i S_j \rangle = \cos[2(t_j - t_i)]$ is independent of the initial state, whether $|N\rangle|0\rangle$ or $|0\rangle|N\rangle$. Choosing $t_1 = 0$, $t_2 = \pi/6$, $t_3 = \pi/3$ (or $t_3 = 5\pi/12$), the quantum prediction is $LG = 1.5$ (1.37), which gives a violation of (1) [2]. We have solved the Hamiltonian (2) for $N = 100$ and $g/\kappa = 1$ (Fig. 1), confirming the ideal correlations that give violation of the Leggett-Garg inequality in this regime.

The oscillation times T_N however are impractically high for proposals based on Rb atoms [29,33,48]. The fragility of the macroscopic superposition state and the measured decoherence times for a BEC suggest such an experiment to be infeasible [49]. It is known, however, that practical oscillation times can be obtained using a different initial state $|N - n_L\rangle|n_L\rangle$ ($0 < n_L < N$), where initially there are atoms in both wells [29,33]. The dynamical solution presented in Fig. 2 with $n_L = 10$ reveals a two-state oscillation over reduced time scales, mimicking the experiment of Albiez *et al.* [29] for $N = 1000$ atoms where coherent oscillations were observed over milliseconds.

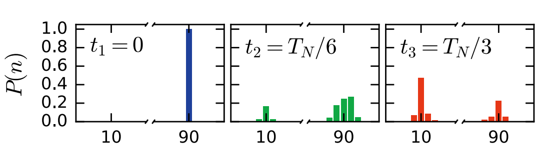

FIG. 2. Mesoscopic two-state oscillations, where $N = 100$, $g/\kappa = 1$. The initial state has 90 atoms in mode a. The Leggett-Garg inequality (1) is violated with $LG = 1.43$, assuming a non-clumsy measurement of S_2 at t_2.

The objective of this paper is to propose strategies for testing Leggett-Garg inequalities in such experiments. There are two questions to be addressed. The first is how to perform (or access the results of) the noninvasive measurement, which is assumed to exist according to the Leggett-Garg premises (NIM). The second is how to test macrorealism when (as in Fig. 2) the values of S_i do not always correspond to macroscopically distinct outcomes.

III. STRATEGIES FOR ACCESSING THE RESULT OF THE NONINVASIVE MEASUREMENT (NIM)

The first question has been discussed quite extensively in the literature [2]. The measurement at t_1 can be made noninvasively by the preparation of a fixed number of particles in each of the modes. The $\langle S_1 S_2 \rangle$ and $\langle S_1 S_3 \rangle$ can hence be inferred using deterministic state preparation and projective measurements at t_2 and t_3, based on the Leggett-Garg premise that the system was in a state with definite S at time t_i, and that the projective measurement will reveal which state the system was in (and hence the value of S_i) [2]. To measure $\langle S_1 S_3 \rangle$ no intervening measurement is made at t_2, based on the assumption that the noninvasive measurement (NIM) at t_2 will not affect the subsequent statistics. For $\langle S_2 S_3 \rangle$, S_3 is measured projectively, but the evaluation of S_2 is difficult, since with any practical measurement it could be argued that a measurement $\hat{M}$ made at t_2 is not the actual noninvasive measurement, and does indeed influence the subsequent dynamics. The following three strategies may be used to counter this objection: (A) Ideal negative-result measurements, (B) minimally invasive (nonclumsy) projective measurements, and (C) weak measurements.

A. Ideal negative-result measurement (INR) strategy

A strong test is possible if the two modes of the NOON superposition (4) correspond (at time t_2) to spatially separated locations. In this case, the INR strategy outlined by Leggett and Garg can be applied. A measurement apparatus at time t_2 couples locally to only one mode a, enabling measurement of the particle number n_a. Either $n_a = 0$ or $n_a = N$. Based on the first Leggett-Garg premise, if one obtains $n_a = 0$, it is assumed that there were prior to the measurement no atoms in the mode a. Hence the measurement that gives a negative result is justified to be noninvasive. The $\langle S_2 S_3 \rangle$ can be evaluated using only negative-result outcomes, as described in Leggett and Garg's original paper [2]. In such an experiment, there is implicit the assumption of locality: that there is no change to one mode because of measurement on the other. In the double-well example, the modes associated with each well can in principle be further separated for the counting measurement on one mode at the time t_2 [29], and recombined for the subsequent evolution (see Sec. IV).

It might be argued (based on experiments that confirm violation of Bell's inequality) that the measurement on one mode *can* induce a nonlocal backaction effect on the macroscopic state of the other mode, so that there may be a change of the state of the second mode of up to δ particles, where $\delta \leqslant N$. The change δ may be microscopic, not great enough to switch the system between macroscopic states at t_2, but might alter the subsequent dynamics, to induce a macroscopic change at t_3. If we assume quantum states at t_2, then changes to the dynamics can be established within quantum mechanics, to give a range of prediction for $\langle S_2 S_3 \rangle$. We have performed this calculation and plot the effect of δ for various N in Fig. 1(c), noting that a moderately small backaction δ to the quantum state of one mode will destroy violations of the Leggett-Garg inequality even for large N.

B. Nonclumsy projective (NCP) measurement strategy

A second strategy constructs a measurement $\hat{M}$ that can be shown to give a negligible disturbance to the system being measured, if it is indeed in one of the two macroscopically distinguishable states [4,17]. This strategy is useful if the modes are co-located or if both modes are occupied at t_2 (as in the experiment of Ref. [29]).

Suppose the state at time t_2 is a superposition

$$|\psi\rangle = c_- |\psi_-\rangle + c_+ |\psi_+\rangle \tag{5}$$

of states $|\psi_+\rangle$ and $|\psi_-\rangle$ that give, respectively, outcomes for $\hat{S}_2$ of $S_2 = \pm 1$. Here $c_\pm$ are probability amplitudes. We apply the Leggett-Garg premises in this case, assuming the two states are macroscopically distinguishable. The first Leggett-Garg premise asserts that the system is in a state of either positive or negative S_i, at any given time t_i. The second premise assumes there is no change to the value of S_3 at t_3, due to the noninvasive measurement (NIM) at t_2.

According to quantum mechanics, an appropriately selected nondestructive projective measurement $\hat{M}$ of $\hat{S}_2$ will not change the state of the system at time t_2 (and hence not change the outcome at time t_3), *if* the system at time t_2 is indeed in one of the states $|\psi_+\rangle$ and $|\psi_-\rangle$ (which are eigenstates of $\hat{S}_2$). Such a measurement is referred to in this paper as a minimally invasive, or "*nonclumsy*", projective (NCP) measurement of $\hat{S}_2$. The INR measurement discussed in Sec. III A is an example of a nonclumsy measurement of $\hat{S}_2$, for systems prepared in the NOON state. The nonclumsy projective (NCP) measurement strategy requires a control experiment, in order to experimentally establish that states with a definite value of S_2 are indeed unchanged by the measurement [4,23]. The noninvasiveness of the measurement is then justified by the first Leggett-Garg premise, that the system is in a state of either positive or negative S_2.

In fact, for any realistic "clumsy" measurement, a small change may arise, which can be experimentally measured. One can experimentally quantify this change, if the system is indeed in one or other of the two macroscopically distinguishable states at t_2, by preparing the system in one or other state, and measuring any change to the dynamics at time t_3 as a consequence of the measurement [4,17,23]. Hence, the NCP strategy is to measure the probabilities $P_\pm$ for the outcomes $S_2 = \pm 1$ respectively. The prediction is $P_\pm = |c_\pm|^2$. Then one prepares the system in the state $|\psi_+\rangle$ at time t_2, measuring S_3 at the later time t_3, without the measurement $\hat{M}$ being made on the state at t_2. This allows measurement of the moment $\langle S_2 S_3 \rangle_+$ where the system at time t_2 is indeed in the state $|\psi_+\rangle$ at time t_2. Similarly, one prepares the system in the state $|\psi_-\rangle$ to measure $\langle S_2 S_3 \rangle_-$. If the Leggett-Garg premises are correct, then the conclusion is that

$$\langle S_2 S_3 \rangle = P_+ \langle S_2 S_3 \rangle_+ + P_- \langle S_2 S_3 \rangle_-, \tag{6}$$

and this is the same result for $\langle S_2 S_3 \rangle$ that is measured using the nonclumsy measurement $\hat{M}$. The measurement of $\langle S_2 S_3 \rangle$ is repeated, but this time with the measurement $\hat{M}$ being made on the prepared state $|\psi_\pm\rangle$ at the time t_2 (prior to the evolution to the later time t_3), to give a moment that we call $\langle S_2 S_3 \rangle_{MC}$. If the measurement $\hat{M}$ is nonclumsy, then $\epsilon \equiv \langle S_2 S_3 \rangle_{MC} - \langle S_2 S_3 \rangle = 0$. The change due to a clumsy measurement can be quantified and thus be accounted for, through extra terms in the inequalities [4,17,23]. This type of experiment has been carried out recently for superconducting circuits [4]. Figure 2 gives predictions of Leggett-Garg violations using such a NCP measurement approach, for the two-well system.

It could be argued that the NCP measurement approach is limited to test a modified Leggett-Garg assumption, that the system is always in a *quantum* state with definite S_2 at the time t_2. This is because of the possibility that the predetermined states (with definite values of S_2) are *hidden variable states*, and are not able to be represented as quantum states. It is therefore difficult to prove that all hidden variable states with definite outcome of S_2 are not changed by the NCP measurement. The individual quantum states $|\psi_\pm\rangle$, on the other hand, can be prepared accurately, and the effectiveness of preparation verified by quantum tomography. An analysis of the different models tested by the Leggett-Garg inequalities is given by Maroney and Timpson [50]. Regardless, if the Leggett-Garg inequalities are violated, the NCP measurement strategy rigorously demonstrates the quantum coherence between the states $|\psi_+\rangle$ and $|\psi_-\rangle$. This is because the Leggett-Garg inequalities cannot be violated if the system, at time t_2, is described probabilisitically as being in one or other of the two states $|\psi_\pm\rangle$.

We now consider a specific quantum model for a nonclumsy projective measurement strategy that applies to the two-well atomic system. The NCP measurement (labeled $\hat{M}$) is modeled by the Hamiltonian

$$H_Q = \hbar G \hat{J}_z \hat{n}_c, \tag{7}$$

which for atomic spin describes a measurement of $\hat{J}_z$ based on an ac Stark shift [51]. An optical "meter" field c is prepared in a coherent state $|\gamma\rangle$ and coupled to the atomic system for a time τ_0. The meter field is a single mode with boson operator $\hat{c}$ and number operator $\hat{n}_c = \hat{c}^\dagger \hat{c}$. The quantum model for this measurement is given in more detail in Refs. [22,51]. Writing the state of the atomic system at time t_2 as $\sum_{m=0}^{N} d_m |m\rangle_a |N-m\rangle_b$ (d_m are probability amplitudes), the output state immediately after measurement is (setting $\tau_0 = \pi/2NG + 2\pi K$ where K is a nonegative integer)

$$|\psi\rangle = \sum_{m=0}^{N} d_m |m\rangle_a |N-m\rangle_b |\gamma e^{i\pi(N-2m)/2N}\rangle_c. \tag{8}$$

Homodyne detection on the optical system enables measurement of the meter quadrature phase amplitude $\hat{p} = (\hat{c} - \hat{c}^\dagger)/i$. For γ large, the different values of $\hat{J}_z$ (and hence $\hat{S}_2$) are measurable by outcomes for $\hat{p}$ and the atomic system after the homodyne measurement collapses to a state of definite J_z. Unless the atomic system is initially in a NOON state, this is a "clumsy" measurement of $\hat{S}_2$. The nonclumsy measurement of $\hat{S}_2$ leaves eigenstates of $\hat{S}_2$ (the sign of the atomic spin $\hat{J}_z$)

unchanged. The nonclumsy measurement thus discriminates only the sign of $\hat{p}$ and collapses the superposition state at time t_2 into one or other state, $|\psi_+\rangle$ or $|\psi_-\rangle$. For the case of Fig. 2, Leggett-Garg violations are predicted, with γ large, for the nonclumsy measurements.

C. Weak measurement strategy

The limit $\gamma \to 0$ of the NCP measurement (7) enables the weak measurement (WM) strategy [11–13,19,21]. Here the *entire* quantum state of the system at t_2 is *undisturbed* by the measurement. If the system at time t_2 is in a NOON state (4), then the relation

$$\langle S_2 S_3\rangle = -\frac{1}{2\gamma}\langle p S_3\rangle \tag{9}$$

holds for all γ. This relation is derived in Ref. [22] and can be experimentally verified for the purpose of a Leggett-Garg test. Although in the weak measurement limit there is no clear resolution of the value S_2 (values can exceed the eigenvalue range [18], a phenomenon known as quantum weak values), the value of $\langle S_2 S_3\rangle$ as given by projective measurements can be obtained by averaging over many runs [11,12]. The term "weak measurement" is here used in the sense of the measurements defined by Aharonov, Albert, and Vaidmann, which yield quantum weak values [18]. This contrasts with measurements weak in the sense of a weak meter-system coupling (e.g., a coupling to only one of many system modes), but that are nonetheless projective measurements collapsing the system into a definite eigenstate [2,7,52].

The weak measurement strategy enables an interesting and important Leggett-Garg test, since one can experimentally demonstrate (independently of the quantum prediction) the *noninvasiveness of the weak measurement*, by showing the invariance of $\langle S_1 S_3\rangle$ as $\gamma \to 0$ when the measurement is performed at t_2. This implies a zero disturbance as $\gamma \to 0$

$$d_\sigma \equiv \langle S_3|\hat{M}_2,\sigma\rangle - \langle S_3|\sigma\rangle = 0, \tag{10}$$

where d_σ is defined in the Introduction. Different to the previous strategies, the *three* measurements can therefore be carried out in a *time-ordered sequence* for each given run: the preparation at time t_1, the weak measurement at time t_2, and the final projective measurement at t_3. This sequence yields for each run the values of the spin products S_1S_2, S_1S_3, and S_2S_3 required for the Leggett-Garg inequality. The moments $\langle S_iS_j\rangle$ are evaluated by averaging over all runs. However, the weak measurement is not an actual measurement of S_2 (because it does not yield the value of S_2 being either $+1$ or -1) and one is surmising the measured $\langle S_2S_3\rangle$ to be that of the noninvasive measurement (NIM), which exists according to the Leggett-Garg premises.

Experiments using a weak measurement strategy to demonstrate violation of Leggett-Garg inequalities have been carried out for systems of a single photon and for superconducting circuits. Violation of the Leggett-Garg inequality in this case is linked to the observation of quantum weak values and occurs only in the weak measurement limit where γ is sufficiently small. The detailed study of quantum weak values for this system has been given in a different paper [22]. This strategy is useful where generalized NOON states are generated at time t_2, and where an INR measurement cannot be performed.

For γ sufficiently large, the weak measurement becomes a projective measurement, and the violation of the Leggett-Garg inequality is lost, if one uses the WM strategy of three successive measurements. This is clear, since the projective measurement will at any time yield the result of either 1 or -1, thus ensuring $LG \leqslant 1$. References [3,22] calculate the threshold $\gamma > 0.52$ for the loss of violation in the ideal case given by Eq. (4), if one chooses $t_1 = 0$, $t_2 = \pi/6$ and $t_3 = 5\pi/12$. For projective measurements, the violation of the Leggett-Garg inequality is achieved using the NCP or INR approaches, where $\langle S_2S_3\rangle$ and/or $\langle S_1S_3\rangle$ is inferred, based on the validity of the Leggett-Garg premises, as described in Secs. III A and III B.

The violation that is possible using projective measurements in one case (NCP or INR strategies), but not the second case (WM strategy), strengthens the argument for failure of the Leggett-Garg premises. The interpretation is that the projective measurement "collapses" the wave function at the time t_2, because, immediately prior to the measurement at time t_2, the system cannot be regarded as being in one state or the other. For systems where the quantum state at time t_2 can be shown to be in a classical mixture of the two states $|\psi_+\rangle$ and $|\psi_-\rangle$, the difference between the two cases does not occur, and there is no violation of the Leggett-Garg inequality.

IV. LEGGETT-GARG TESTS USING INTERFEROMETERS AND THE *s*-SCOPIC LEGGETT-GARG INEQUALITIES

Leggett-Garg tests can be carried out using a nonlinear or linear interferometer. This is depicted schematically in Fig. 3(a). Predictions for violations of Leggett-Garg inequalities using a linear interferometer are given in Figs. 3(b) and 3(c). Figures 2 and 4 show violations using a nonlinear interferometer. In Fig. 3(a), the input state at time t_1 is a two-mode state with N bosons in one mode (implying $S_1 = 1$). The two-mode state undergoes a unitary transformation $BS1$ realized as either a beam splitter (with transmission intensity given by $\cos^2\theta$), or as the nonlinear beam splitter given by the nonlinear Josephson Hamiltonian H_I [Eq. (3)]. After the interaction $BS1$, at time t_2, the sign S_2 of the mode population difference $\hat{J}_z$ may be measured, by the measurement we label $\hat{M}$. Subsequently, the two-mode system evolves according to a further unitary transformation. This is realized as a second nonlinear Josephson interaction H_I, or else as a second beam splitter (BS2, with transmission intensity given by $\cos^2\phi$). The unitary interaction $BS2$ may also be realized as a phase shift ϕ followed by a 50/50 beam splitter. At the output of the interferometer, the population difference $\hat{J}_z$ (and hence S_3) is measured at the final time t_3. A nonlinear interferometer of this type has been realized for atoms in the BEC experiments of Gross *et al.*, based on the interaction H_I [37]. Figure 3(b) (solid blue and red dashed curves) plots predictions for Leggett-Garg tests in the linear case, where $H_I = 0$.

The Leggett-Garg inequalities might also be tested when mesoscopic superposition states are created at a time t_2 as heralded states, produced conditional on a certain outcome being obtained for a preparation measurement $\hat{P}$. For example, the macroscopic Hong-Ou-Mandel technique passes N bosons

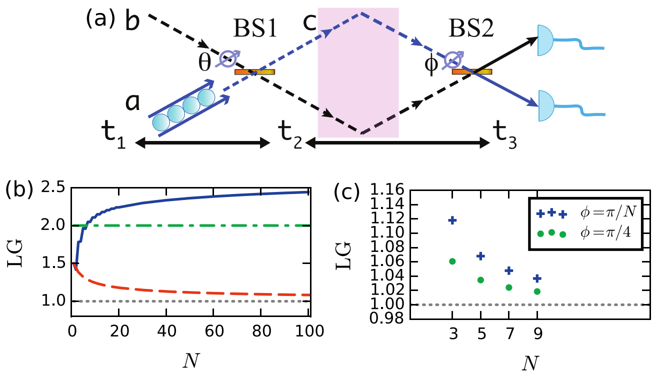

FIG. 3. Leggett-Garg tests using multiparticle interferometers: (a) N bosons pass through an interferometer. A measurement $\hat{M}$ (purple shading) is made on the state created at t_2 and the outgoing fields are combined across a beam splitter $BS2$ with transmission intensity $\cos^2\phi$. J_z of the outputs at time t_3 is measured. (b, c) Results for the case of a simple linear interferometer where the bosonic modes are not coupled by the Josephson nonlinear interaction H_I. The blue solid curve and red dashed curve of (b) plot LG given by (1) for optimal angles θ, ϕ where the state at time t_2 is created by a simple beam splitter $BS1$ (transmission intensity $\cos^2\theta$). The red dashed curve of (b) shows LG for odd N where $\hat{M}$ is a nonclumsy measurement of S_2. The blue solid curve is where $\hat{M}$ measures $\hat{J}_z$ and hence the number of particles in arm c. This is a nonclumsy measurement of S_2 only when the number of particles in each arm is fixed. The green dotted-dashed curve shows the disturbance $d_\sigma = 2$ for optimal angles and N odd, where mesoscopic superposition states $|\psi_\Delta\rangle$ are created at t_2 by conditioning on $|J_Z| > \Delta/2$, as described in the text. Here $\hat{M}$ is a nonclumsy measurement of S_2. The green dotted-dashed curve shows the disturbance d_σ for all values of $\Delta \leqslant N-1$, including where a NOON state is created at t_2. (c) Leggett-Garg where a NOON state is created at t_2, and where the final $BS2$ represents a phase shift ϕ and a 50/50 $BS2$ (for optimal $\tau = \theta$). Here $\hat{M}$ is a nonclumsy measurement of S_2.

through a beam splitter $BS1$ (of transmission intensity $\cos^2\theta$) [26]. A nondestructive measurement is made of $\hat{J}_z$ at the time t_0, and an output state $|\psi_\Delta\rangle$ is then heralded on the result J_z being $|J_z| > \Delta/2$ (here Δ is an integer, $\Delta < N$). This creates at t_2 a mesoscopic superposition

$$|\psi_\Delta\rangle = c_-|\psi_-\rangle + c_+|\psi_+\rangle \tag{11}$$

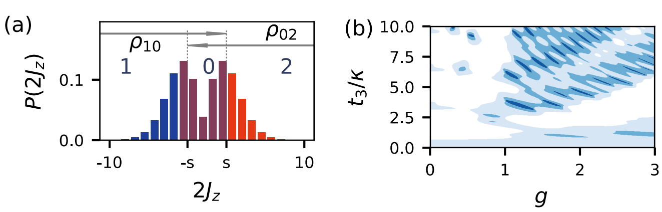

FIG. 4. Violation of s-scopic Leggett-Garg inequalities*:* The NOON state (4) is created at time t_2 ($N = 5, t = \pi/6$) and evolves for a time t_3 according to H_I with nonlinearity g. (Note here we have set $t_2 = 0$ for convenience). (a) Schematic of the probability distribution for results $2J_z$ at t_3. (b) Contours show regimes for violation of the s-scopic inequality (12) with $s = s_2 = s_3$, where (dark to light) $s = 4,2,0$.

of two states $|\psi_+\rangle$ and $|\psi_-\rangle$ that are distinct by $\Delta + 1$ (or more) particles in each arm of a two-mode interferometer [53]. Here $c_\pm$ are probability amplitudes. In this case, the time t_1 that is needed for the Leggett-Garg test is the time t_0, that of the preparation outcome $|J_z| > \Delta/2$. For the heralded state, this outcome is deterministic. Hence S_1 is specified $+1$ if the result of the measurement $\hat{P}$ is $|J_z| > \Delta/2$, and -1 otherwise. For the heralded state, S_1 is always $+1$. We note that for $\Delta = N-1$, a generalized NOON state of type (4) is created by at time t_2 using this method.

Figures 2, 3(b), 3(c), and 4 show predictions for Leggett-Garg violations where a mesoscopic superposition $|\psi_\Delta\rangle$ (or a NOON state) has been created at time t_2, either by the conditional method or by the dynamics H_I. In Figs. 2 and 4, it is supposed that subsequently, after the measurement $\hat{M}$, the system evolves according to the Josephson nonlinear interaction H_I. A measurement $\hat{J}_z$ is then made at t_3. This gives an Leggett-Garg test using a nonlinear interferometer. In Fig. 3(b) (dotted-dashed green curve) and Fig. 3(c), it is supposed that between t_2 and t_3, $H_I = 0$, which corresponds to a linear interferometer.

With these different strategies, however, the outcomes for $\hat{J}_z$ at the times t_3 are not always restricted to $\pm N/2$ [Fig. 4(a)]. Before discussing the implications of the Leggett-Garg violations shown in Figs. 2, 3, and 4, and to fully explore the possibilities for Leggett-Garg tests using interferometers, we address this case by deriving modified Leggett-Garg inequalities. To do this, we expand on previous work [2,54].

A. The s-scopic Leggett-Garg inequalities

We consider a measurement $\hat{J}_z$ made on the system at time t_i and define three regions of outcome: region "1," $J_z < -s_i/2$; region "0," $-s_i/2 \leqslant J_z \leqslant s_i/2$; and region "2," $J_z > s_i/2$. Where the probability P_0 for a result in region 0 is zero, the regions 1 and 2 are distinct by s_i. The premise of *s_i-scopic realism* (s_iR) asserts that the system at time t_i (prior to measurement) is either in a state with an outcome in region "1," or in a state with an outcome in region "2."

Generalizing to $P_0 \neq 0$ [Fig. 4(a)], the meaning of s_iR is that the system at time t_i is in one or other of two *overlapping* states: the first that gives outcomes in regions "1" or "0" (denoted by $\tilde{S} = -1$); the second that gives outcomes in regions "0" or "2" (denoted by $\tilde{S} = 1$) [2,54]. This premise adequately describes quantum superpositions of states that give outcomes of $\hat{J}_z$ different by up to s_i, but not (necessarily) superpositions of states with greater separations. The premise allows for an indeterminacy in the predetermination of the result of a measurement of $\hat{J}_z$ by an amount up to $\sim s_i$, since any such indeterminate state can be described as either $\tilde{S} = 1$ or $\tilde{S} = -1$. Macroscopic superpositions where there is the possibility of interpretation that the system would not comply with this restricted indeterminacy are not (necessarily) consistent with the premise. This approach was suggested originally by Leggett and Garg [2] and has been developed to provide tests of mesoscopic quantum coherence and mesoscopic Bell nonlocality [54,55].

A measurement $\hat{J}_z$ gives the value of $\tilde{S}$ for regions 1 and 2, there being ambiguity only in the region 0. The second Leggett-Garg premise is generalized to *(s_2,s_3)-scopic noninvasive* *measurability* [(s_2,s_3)-NIM]. This premise asserts that such a measurement can be made at t_2, without changing the result J_z at time t_3 by an amount s_3 or more. Any change or back-action due to the measurement by an amount up to s_3 will not alter the recorded value $\tilde{S}$ at time t_3, provided the experimenter takes into account that results in the region 0 cannot be distinguished as being either $\tilde{S} = +1$ or $\tilde{S} = -1$. Combined, we will refer to the s_iR and (s_2,s_3)-NIM premises as the s-scopic Leggett-Garg premises.

The s-scopic Leggett-Garg premises imply a quantifiable inequality, because any effects due to the ambiguous region are limited by the finite probability of observing a result there. Defining the measurable marginal probabilities of obtaining a result in region $j \in \{0,1,2\}$ at the time t_k by $P_j^{(k)}$, the s-scopic premises are violated if

$$LG_s \equiv P_2^{(2)} - P_1^{(2)} + \langle S_2 S_3 \rangle - \left(P_2^{(3)} - P_1^{(3)}\right) - 2P_{0|M}^{(3)} - P_0^{(3)} > 1, \quad (12)$$

where $P_{j|M}^{(3)}$ ($P_j^{(3)}$) is the probability with (without) the measurement M performed at t_2. The details of the derivation are given in Appendix A. We have assumed that the system is prepared initially in region 2 and restrict to scenarios satisfying $P_0^{(2)} = 0$. The $\langle S_2 S_3 \rangle$ is to be measured using a noninvasive measurement at t_2, as described in Sec. III. The $P_j^{(k)}$ are measurable by projective measurements. A similar modification can be given for the disturbance inequality.

B. Nonlinear interferometer

Figures 2 and 4(b) show violations of the s-scopic Leggett-Garg premises for nonzero s, using the nonlinear interaction H_I. In the case given by Fig. 2, we obtain violations of the Leggett-Garg inequality (12) with $s = s_2 = s_3 = 80$. Figure 2 depicts the example of the nonlinear interferometer where the parameters N, g, κ and the initial condition are selected to maintain a mesoscopic superposition throughout the evolution. Josephson oscillations similar to this have been realized in the experiments of Albiez *et al.* based on a BEC with Rb atoms [29]. A relevant measure of macroscopicity in this case is the mass difference given by sm_A (in each mode) of the two states forming the superposition, m_A being the mass of each atom. Figure 4(b) shows the violation of the s-scopic Leggett-Garg inequalities for smaller N, where the NOON state ($N = 5$) is created at time t_2, followed by evolution according to the nonlinear Hamiltonian H_I until time t_3. Here the state created at t_3 need not be a NOON state, depending on the value of g.

C. Linear interferometer

Leggett-Garg tests are also possible where $H_I = 0$ (Fig. 3). First, we consider the simplest case depicted by the diagram of Fig. 3(a), where an N-boson state at time t_2 is created by the simple beam splitter $BS1$ (transmission intensity $\cos^2\theta$), or alternatively a polarizer beam splitter rotated at angle θ. Here it is possible to test the hypothesis of individual classical trajectories for the bosons traveling through the linear interferometer.

At time t_1, N bosons are prepared in the single mode a. After t_1, the N bosons pass through the polarizer beam splitter (or equivalent) ($BS1$) rotated at angle θ. For the evaluation of $\langle S_2 S_3 \rangle$, a nondestructive measurement $\hat{M}$ of J_z is made at time t_2. The number difference J_z indicates the value of J_θ (and hence S_2) at t_2. The spin S_i is defined as in Sec. II at each time t_i to be the sign of J_z. The outgoing particles are then incident on a second polarizer beam splitter $BS2$ at angle ϕ (or alternatively, a beam splitter with transmission intensity $\cos^2\phi$) whose output number difference J_z gives J_ϕ and hence S_3 at t_3. We invoke the Leggett-Garg premise, that the system is always in a state of definite J_z immediately prior to the measurement $\hat{M}$ at t_2. This is based on the hypothesis that *each* atom (boson) goes one way *or* the other, through the paths of the interferometer. A second Leggett-Garg premise is invoked, that a measurement $\hat{M}$ could be performed of J_z at t_2 that does not disturb the subsequent evolution. The second premise can be supported by experiments that create a spin eigenstate, and then demonstrate the invariance of the state after the number measurement $\hat{M}$. If the premises are valid, the Leggett-Garg inequalities (1) will hold, but by contrast are predicted violated by quantum mechanics (Fig. 3(b), blue solid curve). We assume fixed number inputs, achievable for photons [11] and likely in the future for atoms given the recent demonstrations of quantum correlated atomic beams [27,56].

For this case, the violation is given only for $s = 0$, and NOON states are not created at the time t_2. While not the macroscopic test Leggett and Garg envisaged, this nonetheless allows a test of the "classical trajectories" hypothesis that can be applied to atoms in a two-mode interferometer [37,38,49]. The violation of the Leggett-Garg inequality demonstrates the absence of individual classical trajectories, as in *each* atom passing through one arm or mode of the interferometer. Potential loopholes associated with the second premise are as for the NCP measurement strategy, discussed in Sec. III B and in the Conclusion. The details of the calculations are given in Appendices B and C, which include a table of the angles θ and ϕ required for the maximum violation.

The same experiment can be performed with a nonclumsy measurement $\hat{M}$ of S at time t_2. This corresponds to detecting the sign of the outcome for $\hat{J}_z$ at time t_2, without projecting the state into individual eigenstates of $\hat{J}_z$. Rather, the system after measurement is collapsed into the one of the states $|\psi\rangle_+$ or $|\psi_-\rangle$ which have a non-negative or negative outcome for $\hat{J}_z$ respectively. Such an experiment tests the following Leggett-Garg premises: the system is at any given time in one of the states $|\psi_+\rangle$ or $|\psi_-\rangle$ prior to measurement, and the measurement M does not influence the dynamics to the extent that the state of the system is changed from $|\psi_+\rangle$ to $|\psi_-\rangle$ (vice versa) at the time t_3. We see from the results plotted by the red dashed curve of Fig. 3(b) that Leggett-Garg violations are possible (for $s = 0$). Here the two states $|\psi_\pm\rangle$ are not mesoscopically distinct, except in the limit of $N \to \infty$ where the violation vanishes ($LG \to 1$). Violations of the s-scopic Leggett-Garg inequalities with $s > 0$ are not given in this case.

Where a NOON state is prepared at time t_2 and there is a spatial separation of the two trajectories at that time, stronger Leggett-Garg tests are possible. This is because the assumption of noninvasiveness of the measurement $\hat{M}$ at time t_2 can be strengthened by using an INR method (refer to Sec. II). Violations of the Leggett-Garg inequality are shown for this case in Figs. 3(b) and 3(c). The green dashed curve of Fig. 3(b) shows $d_\sigma = 2$. This implies violation of the disturbance equality (2), where the mesoscopic superposition $|\psi_\Delta\rangle$ of Eq. (11) is created at time t_2, and where the measurement at time t_3 is of J_ϕ, defined in the second paragraph of this subsection. The detailed calculations are given in Appendix C. Similar violations are possible for the Leggett-Garg inequality (1), with the calculations also given in Appendix C. We see from those calculations that the violations of the Leggett-Garg inequality (1) are enhanced where a NOON state is created at the time t_2, the violations increasing with N, for odd N. Figure 3(c) shows violations of the Leggett-Garg inequality where a NOON state is created at time t_2, but where the measurement at time t_3 is replaced with the phase shift ϕ followed by a beam splitter. Violations are obtained with $s_2 = N$. All violations shown in Fig. 3 are, however, for $s_3 = 0$. Details of the calculations are provided in Appendix D.

V. CONCLUSION

In this paper, we have developed strategies for tests of Leggett and Garg's mesoscopic realism using multiparticle interferometers, based on the nonlinear Josephson interaction model H_I. By deriving modified inequalities that apply where not all outcomes are mesoscopically distinct, we find the tests are enhanced over a wider range of parameter values. The interaction H_I is fundamental not only to Bose-Einstein condensates but describes Josephson effects in superconductors [45], superfluids [46], and, more recently, exciton polaritons [47]. We have also proposed tests of Leggett-Garg realism at a microscopic level suitable for application to multiparticle linear interferometers where $H_I = 0$.

Finally, to conclude the paper, we summarize potential loopholes for the strategies outlined in this paper. For the INR and NCP strategies given in Secs. III A and III B, the violation of macrorealism arises in effect because the value of $\langle S_1 S_3\rangle$ depends on whether the measurement $\hat{M}$ is made at time t_2. Specifically, the disturbance d_σ defined by Eq. (2) is nonzero. These tests are therefore only convincing when the measurement $\hat{M}$ that is used to evaluate the $\langle S_2 S_3\rangle$ can be justified as macroscopically noninvasive. The macrorealist, who believes the system is always in one of two macroscopically distinguishable states ψ_+ and ψ_-, will most likely challenge this justification.

For the NCP strategy of Sec. III B, the noninvasiveness of $\hat{M}$ is justified by preparing the system in the states $\psi_\pm$ and demonstrating no-disturbance $d_\sigma = 0$ in each case. Assuming the quantum states $|\psi_\pm\rangle$ can be reliably prepared, the violation of the Leggett-Garg inequality using this strategy then gives a convincing demonstration that the system is not in one or other of the quantum states $|\psi_\pm\rangle$ at the given time. The experiment thus demonstrates macroscopic quantum coherence: the system is not in a classical mixture of the states $|\psi_\pm\rangle$. However, the macrorealist is not restricted to quantum mechanics and would be ready to consider alternative descriptions of $\psi_\pm$ that are consistent with macrorealism. The macrorealist may argue that alternative (nonquantum) realizations of the states $\psi_\pm$ exist, the measurement $\hat{M}$ being invasive for such a realization. A related loophole is the difficulty of preparing all realizations of the macroscopic state $\psi_\pm$, this being a many-body state for which there can be many microscopically different realizations possessing the same value for a macroscopic parameter. The macrorealist may also argue that the system at time t_2 is in a state *microscopically different* to either $|\psi_+\rangle$ or $|\psi_-\rangle$, the measurement $\hat{M}$ being microscopically invasive for this state (causing the collapse to $|\psi_+\rangle$ or $|\psi_-\rangle$). The microscopic change at time t_2 brought about by $\hat{M}$ may lead to a macroscopic change at time t_3, thus explaining the violation of the Leggett-Garg inequality in a way that is consistent with macrorealism. In short, the macrorealist would want to be convinced that the experimentalist can prepare all relevant quantum (and nonquantum) states for the test of nonclumsiness of the measurement.

The weak measurement (WM) strategy in Sec. III C has the advantage that justification of noninvasiveness is not required, the disturbance d_σ being zero in the ideal limiting case of a weak measurement. The smallness of d_σ ($d_\sigma \to 0$) is verifiable experimentally. There is no need to assume anything about the nature of the state at time t_2 to demonstrate the noninvasiveness. Rather, the test of macrorealism uses the Leggett-Garg inequality for three sequential measurements. The spins S_1, S_2, and S_3 are measured consecutively for each run, and the moment $\langle S_2 S_3\rangle$ is verifiable as that given by strong measurements. The macrorealist is left to argue that, being an ineffectual measurement of S_2 (that does not yield a value of $+1$ or -1 for a given run), the weak measurement is not the noninvasive measurement implied by the Leggett-Garg NIM premise.

In our view, the INR strategy given in Sec. III A, based on a spatial separation of the modes, provides the strongest test of macrorealism. This strategy does not rely on the re-creation of the states $\psi_\pm$ for demonstrating noninvasiveness. Rather, the assumption of noninvasiveness is based on the assumption of locality. However, local realism has been shown to fail for microscopic systems, and the macrorealist would likely argue that the measurement $\hat{M}$ does indeed cause a nonlocal *microscopic* change to the system at the second location. The macrorealist would argue that this microscopic change at time t_2 leads to a macroscopic change at time t_3, thus explaining the violation of the Leggett-Garg inequality consistently with macrorealism. The realist's argument, however, relies on more macroscopic aspects of nonlocality for atomic systems that have not yet been verified.

ACKNOWLEDGMENTS

We thank P. Drummond and R. Y. Teh for stimulating discussions. This research was supported by the Australian Research Council under Grant No. DP140104584. This work as performed in part at the Aspen Center for Physics, which is supported by National Science Foundation Grant No. PHY-1607611.

APPENDIX A: DERIVATION OF s-SCOPIC LEGGETT-GARG INEQUALITIES

According to the premise sR, the system can be described by a model in which the system is in one of the states $\tilde{S} = -1$ or $\tilde{S} = +1$ at each t_i. We denote the probability of the system being in state $\tilde{S} = +1$ (-1) at a given time by $\tilde{P}_+$ $(\tilde{P}_-)$, noting that $\tilde{P}_+ + \tilde{P}_- = 1$. This defines a sequence of values $\tilde{S}_i$ such that the values are unchanged by the sNIM. Following the original derivation of Leggett-Garg inequality (1), this leads to $-3 \leqslant \tilde{S}_1\tilde{S}_2 + \tilde{S}_2\tilde{S}_3 - \tilde{S}_1\tilde{S}_3 \leqslant 1$. Thus, where $K_{ij} = \langle \tilde{S}_i\tilde{S}_j\rangle$, the inequality $K_{12} - K_{13} + K_{23} \leqslant 1$ of the form (1) holds.

However, the moments $\langle K_i K_j\rangle$ are not *directly* measurable, because an outcome between $-s/2$ and $+s/2$ could ambiguously arise from either state, $\tilde{S} = -1$ or $+1$. Regardless, $P_1 \leqslant \tilde{P}_- \leqslant P_1 + P_0$ and $P_2 \leqslant \tilde{P}_+ \leqslant P_2 + P_0$, where P_1, P_2, and P_0 are the measurable probabilities of obtaining a result for J_z in regions 1, 2, and 0, respectively. Hence, we are able to establish bounds on the two-time moments if the P_0 are measured. The modified inequality is

$$LG_s = K_{12}^{\text{lower}} + K_{23}^{\text{lower}} - K_{13}^{\text{upper}} \leqslant 1. \tag{A1}$$

Here K_{ij}^{lower} is a lower bound to K_{ij}, and K_{ij}^{upper} is an upper bound to K_{ij}. We see that suitable such bounds are given by $K_{ij}^{\text{lower}} = P_{2,2}(t_i,t_j) + P_{1,1}(t_i,t_j) - P_{10,20}(t_i,t_j) - P_{20,10}(t_i,t_j)$ and $K_{ij}^{\text{upper}} = P_{20,20}(t_i,t_j) + P_{10,10}(t_i,t_j) - P_{1,2}(t_i,t_j) - P_{2,1}(t_i,t_j)$. We introduce the notation that $P_{20,10}(t_1,t_2)$, for example, is the joint probability of an outcome J_z in regions 2 or 0 at time t_1, and an outcome J_z in regions 1 or 0 at time t_2.

It is assumed that a measurement has been made of the moment $\langle S_2S_3\rangle$ where S_j is determined by the sign of J_z at time t_j. For example, the moment $\langle S_2S_3\rangle$ can be measured using a weak measurement at time t_2. Alternatively, the moment might be evaluated using the INR method. We wish to express the inequality (A1) in terms of this moment. We proceed by noting the following relations:

$$\begin{aligned} K_{23}^{\text{lower}} &= \langle S_2S_3\rangle - 2P_0^{(2)} - 2P_{0|M}^{(3)},\\ K_{13}^{\text{upper}} &= P_0^{(3)} + P_2^{(3)} - P_1^{(3)},\\ K_{12}^{\text{lower}} &= P_2^{(2)} - P_1^{(2)} - P_0^{(2)}. \end{aligned} \tag{A2}$$

Here $P_j^{(k)}$ is the probability of an outcome for J_z in region j $(j = 0,1,2)$ at the time t_k. We denote $P_{0|M}^{(3)}$ $(P_0^{(3)})$ as the probability of a result in the region 0 at t_3 if the measurement $\hat{M}$ is performed (or not performed) at t_2. We note that the $P_0^{(3)}$ and $P_{0|M}^{(3)}$ can be evaluated experimentally for a particular $\hat{M}$. For the weak measurement as $\gamma \to 0$ the difference between $P_0^{(3)}$ and $P_{0|M}^{(3)}$ becomes zero.

Using the above results and the LG_S inequality defined by Eq. (A1), we obtain

$$\begin{aligned} LG_s \equiv{}& P_2^{(2)} - P_1^{(2)} - (P_2^{(3)} - P_1^{(3)}) + \langle S_2S_3\rangle\\ &-3P_0^{(2)} - 2P_{0|M}^{(3)} - P_0^{(3)} \leqslant 1, \end{aligned} \tag{A3}$$

which reduces to Eq. (12). The proof is given below.

Proof. First, we prove $K_{23}^{\text{lower}} = \langle S_2S_3\rangle - 2P_0^{(2)} - 2P_0^{(3)}$. We note $K_{23} = P(+,+) + P(-,-) - P(+,-) - P(-,+)$ where $P(i,j)$ is the joint probability the system is in state i and j at times t_2 and t_3, respectively, and $+$ and $-$ are the states with $\tilde{S} = +1$ and -1. Hence

$$\begin{aligned} K_{23} ={}& P_{2,2} + P_{0|+,0|+} + P_{0|+,2} + P_{2,0|+}\\ &+P_{1,1} + P_{0|-,1} + P_{1,0|-} + P_{0|-,0|-}\\ &-P_{1,2} - P_{0|-,2} - P_{0|-,0|+} - P_{1,0|+}\\ &-P_{2,1} - P_{2,0|-} - P_{0|+,0|-} - P_{0|+,1}. \end{aligned} \tag{A4}$$

Here $P_{2,2}$ is the joint probability of a result in region 2 at times t_2 and t_3. $P_{0|+,1}$ is the joint probability of an outcome at time t_1 in the region 0, given the system is in the state $+$ (at time t_1), and an outcome in region $+1$ at time t_3. The remaining probabilities are defined similarly. Defining $\langle S_2^+S_3^+\rangle = P_{2,2} + P_{1,1} - P_{1,2} - P_{2,1}$ and simplifying we obtain

$$\begin{aligned} K_{23} \geqslant{}& \langle S_2^+S_3^+\rangle - P_{0|-,2} - P_{0|-,0|+} - P_{1,0|+} - P_{2,0|-}\\ &-P_{0|+,0|-} - P_{0|+,1}\\ \geqslant{}& \langle S_2^+S_3^+\rangle - P_{0|-}^{(2)} - P_{0|+}^{(2)} - P_{0|+}^{(3)} - P_{0|-}^{(3)}\\ \geqslant{}& \langle S_2^+S_3^+\rangle - P_0^{(2)} - P_0^{(3)}. \end{aligned} \tag{A5}$$

Here $P_{0|(\pm)}^{(k)}$ is the probability of an outcome in the region 0 given the system is in the state $(\pm)$ at time t_k. $P_0^{(k)}$ is the probability of an outcome in region 0 at time t_k. Now we note that the measurable moment is

$$\begin{aligned} \langle S_2S_3\rangle ={}& P_{2,2} + P_{0+,0+} + P_{0+,2} + P_{2,0+}\\ &+P_{1,1} + P_{0-,1} + P_{1,0-} + P_{0-,0-}\\ &-P_{1,2} - P_{0-,2} - P_{0-,0+} - P_{1,0+}\\ &-P_{2,1} - P_{2,0-} - P_{0+,0-} - P_{0+,1}, \end{aligned} \tag{A6}$$

where $P_{0+,0+}$ is the probability of a positive outcome in region 0 for both times. The other probabilities are defined similarly. Then we simplify

$$\begin{aligned} \langle S_2S_3\rangle ={}& \langle S_2^+S_3^+\rangle + P_{0+,0+} + P_{0+,2} + P_{2,0+} + P_{0-,1}\\ &+P_{1,0-} + P_{0-,0-} - P_{0-,2} - P_{0-,0+} - P_{1,0+}\\ &-P_{2,0-} - P_{0+,0-} - P_{0+,1}\\ \leqslant{}& \langle S_2^+S_3^+\rangle + P_{0+,0+} + P_{0+,2} + P_{2,0+} + P_{0-,1}\\ &+P_{1,0-} + P_{0-,0-}\\ \leqslant{}& \langle S_2^+S_3^+\rangle + P_{0+}^{(2)} + P_{0+}^{(3)} + P_{0-}^{(2)} + P_{0-}^{(3)}\\ \leqslant{}& \langle S_2^+S_3^+\rangle + P_0^{(2)} + P_0^{(3)}. \end{aligned} \tag{A7}$$

Hence, we obtain the result $K_{23} \geqslant \langle S_2S_3\rangle - 2P_0^{(2)} - 2P_0^{(3)}$ where $P_0^{(k)}$ is the probability of an outcome in region 0 at time t_k. From this we obtain that $K_{23}^{\text{lower}} = \langle S_2S_3\rangle - 2P_0^{(2)} - 2P_{0|M}^{(3)}$ where we have inserted the $|M$ to remind us that the marginal probabilities of a result in the regions at time t_3 in this case are taken after the measurement $\hat{M}$ at time t_2.

We next consider K_{13}. Here we wish to prove that $K_{13}^{\text{upper}} = P_0^{(3)} + P_2^{(3)} - P_1^{(3)}$. This can be done using projective measurements. We see from above that $K_{ij}^{\text{upper}} = P_{20,20}(t_i,t_j) + P_{10,10}(t_i,t_j) - P_{1,2}(t_i,t_j) - P_{2,1}(t_i,t_j)$. Here $K_{13}^{\text{upper}} = P_{20,20}(t_1,t_3) + P_{10,10}(t_1,t_3) - P_{1,2}(t_1,t_3) - P_{2,1}(t_1,t_3)$, which reduces to

$$K_{13}^{\text{upper}} = P_0^{(3)} + P_2^{(3)} - P_1^{(3)}, \tag{A8}$$

where we have used that the system at t_1 is initially prepared in region 2, so that $P_2^{(1)} = 1$. Here we infer that the measurement at time t_3 is made without the measurement $\hat{M}$ at t_2.

Similarly, we next consider K_{12}. We have from above that $K_{ij}^{\text{lower}} = P_{2,2}(t_i,t_j) + P_{1,1}(t_i,t_j) - P_{10,20}(t_i,t_j) - P_{20,10}(t_i,t_j)$, which implies $K_{12}^{\text{lower}} = P_{2,2}(t_1,t_2) + P_{1,1}(t_1,t_2) -$

$P_{10,20}(t_1,t_2) - P_{20,10}(t_1,t_2)$. This reduces to

$$K_{12}^{\mathrm{lower}} = P_2^{(2)} - P_1^{(2)} - P_0^{(2)}. \tag{A9}$$

Thus, using the above results, and applying the LG_s inequality given in Eq. (A1), we obtain the required result (A3).

APPENDIX B: N BOSONS THROUGH A LINEAR INTERFEROMETER

We give details of the proposal of Fig. 3(a) where results are shown by blue solid curve of Fig. 3(b). In this case, there is no nonlinear Hamiltonian evolution. The particles travel through two successive polarizer beam splitters (PBSs). The first beam splitter is set at angle θ. A measurement can then be made of the two-mode number difference, defined as

$$\hat{J}_\theta(t_2) = (\hat{c}^\dagger\hat{c} - \hat{d}^\dagger\hat{d})/2 = \hat{J}_z\cos 2\theta + \hat{J}_x\sin 2\theta. \tag{B1}$$

The normalized $\hat{S}_2 = \hat{J}_\theta(t_2)/(N/2)$ gives the value of the Leggett-Garg observable $\hat{S}_2$. The PBS measurement can be realized by different physical means, including using a PBS (with phase shifts) followed by a photon difference measurement, or, for atom interferometers, as a Rabi rotation followed by an atom number-difference measurement [37,57,58]. Here $\hat{J}_z$ and $\hat{J}_x$ are defined in terms of the initial modes $\hat{a}$ and $\hat{b}$ [e.g., $\hat{J}_z = (\hat{a}^\dagger\hat{a} - \hat{b}^\dagger\hat{b})/2$], and the rotated operators are given by

$$\begin{aligned}\hat{c} &= \hat{a}\cos\theta + \hat{b}\sin\theta,\\ \hat{d} &= -\hat{a}\sin\theta + \hat{b}\cos\theta.\end{aligned} \tag{B2}$$

The measurement $\hat{M}$ of the number difference $(\hat{c}^\dagger\hat{c} - \hat{d}^\dagger\hat{d})/2$ is made at time t_2 after the rotation denoted by θ (achieved by the PBS). In terms of the Leggett-Garg inequality, the rotation denoted by θ in the linear proposal plays the role of the evolution denoted by t_2 in the nonlinear proposal. A subsequent similar rotation (denoted ϕ) and number measurement at time t_3 gives the outcome $\hat{S}_3 = \hat{J}_\phi(t_2)/(N/2)$ as illustrated in Fig. 3(a).

We suppose the initial state is the two-mode number state $|N\rangle_a|0\rangle_b$. The output state at time t_2 after the first beam splitter with rotation θ is

$$|N\rangle_a|0\rangle_b \to \sum_{n=0}^{N} c_n|n\rangle_c|N-n\rangle_d, \tag{B3}$$

where

$$c_n = \sqrt{\frac{N!}{n!(N-n)!}}\cos^n\theta(-\sin\theta)^{N-n}. \tag{B4}$$

After the second beam splitter with rotation ϕ, the output state (in terms of the output modes we call the $\hat{e}$ and $\hat{f}$ modes) is (assuming no measurement $\hat{M}$ is made at t_2)

$$|N\rangle_a|0\rangle_b \to \sum_{n=0}^{N} c_n \sum_{p=0}^{N} c_p^{(n)}|p\rangle_e|N-p\rangle_f, \tag{B5}$$

where

$$c_p^{(n)} = \sum_{k=\max(0,p-n)}^{\min(N-n,p)} \frac{\sqrt{n!(N-n)!}\sqrt{(N-p)!}\sqrt{p!}}{(p-k)!(n-p+k)!k!(N-n-k)!} \times(-1)^{n-p+k}\{\cos^{(N-n+p-2k)}\phi\sin^{(n-p+2k)}\phi\}. \tag{B6}$$

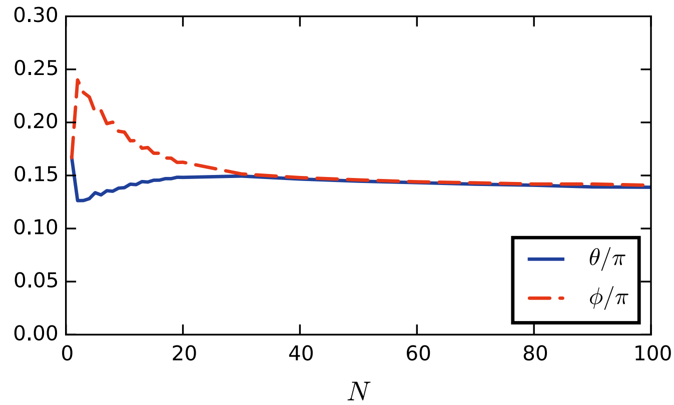

FIG. 5. The optimal angles $\theta_{\max}$ (solid blue line) and $\phi_{\max}$ (dashed red line) that maximize the Leggett-Garg inequality for different values of N.

Calculation gives

$$\begin{aligned}\langle S_1S_2\rangle &= \sum_{n=0}^{N}\mathrm{sgn}(2n-N)c_n^2,\\ \langle S_1S_3\rangle &= \sum_{p=0}^{N}\mathrm{sgn}(2p-N)\left(\sum_{n=0}^{N}c_nc_p^{(n)}\right)^2,\\ \langle S_2S_3\rangle &= \sum_{n=0}^{N}\mathrm{sgn}(2n-N)c_n^2\sum_{p=0}^{N}\mathrm{sgn}(2p-N)\big(c_p^{(n)}\big)^2,\end{aligned} \tag{B7}$$

where $\mathrm{sgn}(x) = 1$ if $x \geqslant 0$ and -1 of $x < 0$. The calculation of $\langle S_2S_3\rangle$ assumes the collapse of the wave function at time t_2 due to the projective measurement of $\hat{J}_z$ at t_2. The moment is then calculated as the weighted average of the individual moments based on all the possible projected eigenstates of $\hat{J}_z$ (number), which are then the initial states for the second PBS.

Using the above results, we maximize the Leggett-Garg inequality violation and obtain the corresponding optimal angles $\theta_{\max}$ and $\phi_{\max}$. Results are shown in Fig. 3(b) (blue solid curve) and Fig. 5.

To understand the nature of the Leggett-Garg violations in the linear case, we plot the probability distributions for the outcome J_z at the different times t. We assume the measurement of $\hat{S}_2$ is made as a nondestructive projective measurement of $\hat{J}_z$. The measurement if made at time t_2 thus collapses the state into the associated two-mode number state. For $N=50$ the optimal angles are $\theta = 0.14518\pi$, $\phi = 0.14522\pi$. After the rotation $BS1$ with θ, the state created at time t_2 has the number distribution plotted in the top graph of Fig. 6. This corresponds to $\langle S_1S_2\rangle = 1$. After the rotation with $\theta+\phi$, the state created at time t_3 has the number distribution plotted in the middle graph of Fig. 6. This corresponds to $\langle S_2S_3\rangle = -0.927$. After the measurement at t_2, the resulting collapsed state is passed through the interferometer with angle ϕ. The number distributions at time t_3 for the three different collapsed states are plotted in the lower graph. Here we take the three most likely measurement results at time t_2 ($n=41$ is the most likely, as shown in the top figure). The correlations for the three cases are $n=40$, $p(n) = 0.139022426845$, $\langle S_2S_3\rangle = 0.39867944914$; $n = 41$,

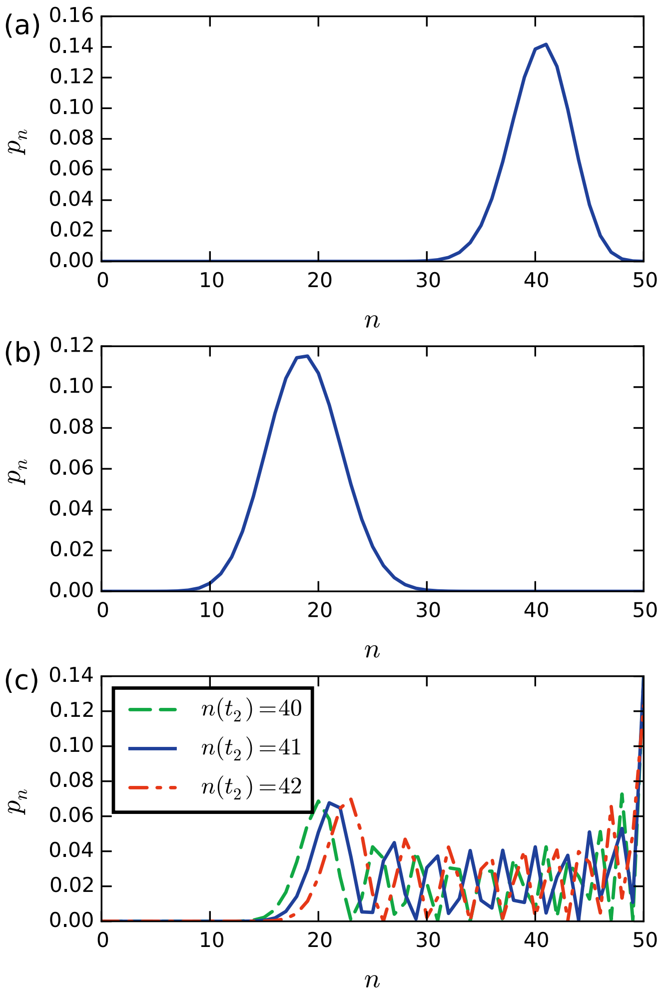

FIG. 6. Plots of the probability distributions of number $n = J_z + N/2$ at the time t_2 (top), and at t_3 if a measurement is made at t_2 (lower) or if not (middle). Here $N = 50$ (the total particles in the interferometer), and n is the number of particles in one arm. The lower graph plots the distributions given that at time t_2 a measurement of n is performed with the outcome $n = 40$ (dashed green line), $n = 41$ (solid blue line), or $n = 42$ (dash-dotted red line).

$p(n) = 0.140876075688$, $\langle S_2S_3\rangle = 0.440046798966$; $n = 42$, $p(n) = 0.125419972345$, $\langle S_2S_3\rangle = 0.442832855968$. Here $p(n)$ is the probability of the result n at the time t_2. The total correlation averaged over all outcomes is $\langle S_2S_3\rangle = 0.434$ and the Leggett-Garg violation is $LG = 2.361$.

APPENDIX C: MESOSCOPIC SUPERPOSITION AT TIME t_2 IN A LINEAR INTERFEROMETER

We suppose we create at time t_2 a superposition of two states $|\psi_+\rangle$ and $|\psi_-\rangle$ mesoscopically distinct (at time t_2), using, for example, a macroscopic Hong-Ou-Mandel effect. This effect employs a conditional measurement to create a mesoscopic superposition. We first evaluate the output state as created from the beam splitter $BS1$. We write the output state as a superposition $\psi = \sqrt{P_-}|\psi_-\rangle + \sqrt{P_0}|\psi_0\rangle + \sqrt{P_+}|\psi_+\rangle$ of three states defined by a positive parameter Δ that specifies a middle region of J_z of width Δ and centered about 0. Here $|\psi_\pm\rangle$ has outcomes J_z in region $J_z > \Delta/2$ and $J_z < -\Delta/2$, respectively, and $|\psi_0\rangle$ is a central state where outcomes for J_z satisfy $|J_z| \leqslant \Delta/2$. Here

$$|\psi_j\rangle = \frac{1}{\sqrt{P_j}} \sum_{n\in R_j(\Delta)} c_n |n\rangle_c |N-n\rangle_d, \tag{C1}$$

where $j \in \{-,+,0\}$, $P_j = \sum_{n\in R_j} |c_n|^2$, and the regions are defined as $R_-(\Delta) = \{2n < N - \Delta\}$, $R_+(\Delta) = \{2n > N + \Delta\}$, $R_0(\Delta) = \{N - \Delta \leqslant 2n \leqslant N + \Delta\}$. The coefficients c_n are given in Eq. (B4). Before time t_2 (at a time we call t_1) a measurement is made that determines whether $|J_z|$ is in the central region or not. We assume this is a nonclumsy measurement, in the sense that the superposition state

$$|\psi_\Delta\rangle = \frac{1}{\sqrt{P_- + P_+}} (\sqrt{P_-}|\psi_-\rangle + \sqrt{P_+}|\psi_+\rangle) \tag{C2}$$

is prepared at the time t_1, by conditioning the future evolution on an outcome $|J_z| > \Delta/2$ at time t_1. With this preparation, the result for S_1 is always 1. Note the time t_1 is defined differently to the above proposals, where the time t_1 refers to the preparation of N particles in the interferometer and no other conditional measurements are made.

1. Evaluation of the Leggett-Garg inequality

First, we evaluate

$$\langle S_1S_2\rangle = \frac{P_+ - P_-}{P_+ + P_-}. \tag{C3}$$

A measurement of S_2 at time t_2 is made on the state $|\psi_\Delta\rangle$, to determine whether the system is in state $|\psi_+\rangle$ or state $|\psi_-\rangle$ (according to the Leggett-Garg premise). The nonclumsy measurement of S_2 corresponds to a measurement at t_2 that measures S_2 but does not resolve the precise number. To perform the calculation of $\langle S_2S_3\rangle$, we consider the system has collapsed to either $|\psi_+\rangle$ (if the result at t_2 is $S_2 = +1$) or $|\psi_-\rangle$ (if the result at t_2 is $S_2 = -1$). At time t_3 the final state for each of the functions $|\psi\rangle_\pm$ is given by

$$|\psi(t_3)\rangle_j = \sum_{n\in R_j(\Delta)} \frac{c_n}{\sqrt{P_j}} \sum_{p=0}^{N} c_p^{(n)} |p\rangle_e |N-p\rangle_f. \tag{C4}$$

Here the coefficients $c_p^{(n)}$ are given in Eq. (B6). Using these values we find

$$\begin{aligned}\langle S_2S_3\rangle &= \frac{P_+}{P_+ + P_-}\langle S_2S_3\rangle_+ + \frac{P_-}{P_+ + P_-}\langle S_2S_3\rangle_- \\ &= \frac{P_+}{P_+ + P_-}\langle S_3\rangle_+ - \frac{P_-}{P_+ + P_-}\langle S_3\rangle_-, \end{aligned} \tag{C5}$$

where $\langle S_3\rangle_\pm$ is the expectation value of S_3 at the time t_3 after the passage through the second $BS2$ set at angle ϕ, given the input state to the second beam splitter $BS2$ is $|\psi\rangle_\pm$. We note that

$$\langle S_2S_3\rangle = \frac{1}{P_+ + P_-}\left[\sum_{p=0}^{N}\left(\sum_{n\in R_+(\Delta)} c_n c_p^{(n)}\right)^2 - \sum_{p=0}^{N}\left(\sum_{n\in R_-(\Delta)} c_n c_p^{(n)}\right)^2\right].$$

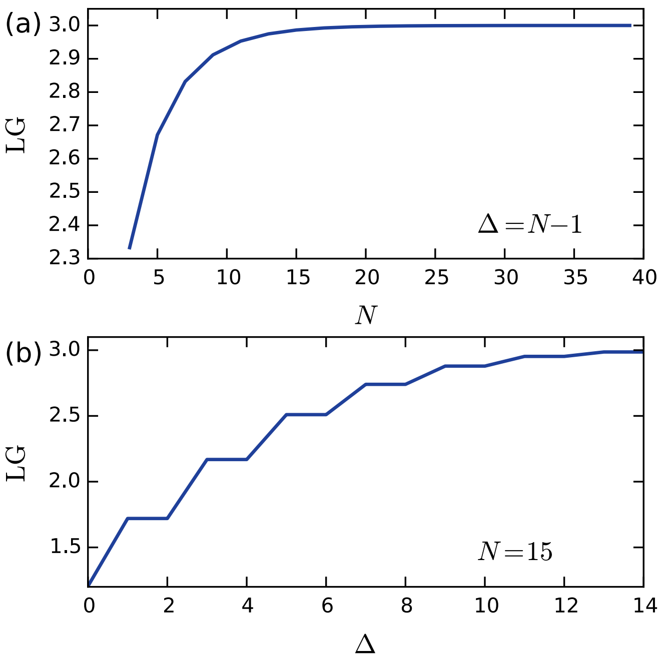

FIG. 7. The top graph shows the violation of the Leggett-Garg inequality (1), as described in the text, for odd N and for the optimal choice of Δ and angles θ and ϕ. The optimal violation is achieved when the NOON state is created at time t_2. The lower graph shows the LG value for $N = 15$, versus Δ.

Here $R_-(\Delta) = \{2n < N - \Delta\}$, $R_+(\Delta) = \{2n > N + \Delta\}$, $R_0(\Delta) = \{N - \Delta \leqslant 2n \leqslant N + \Delta\}$.

The moment $\langle S_1 S_3\rangle$ is evaluated without the measurement $\hat{S}_2$ at t_2, based on the superposition $|\psi_\Delta\rangle$ created at time t_1. This means we evaluate the expectation value of S_3 after a rotation given by beam splitter BS2 set at angle ϕ, for the full input state $|\psi_\Delta\rangle$.

The violation of the Leggett-Garg inequality (1) with no conditioning ($\Delta = 0$) is shown by the red dashed curve in Fig. 3. The violations improve for nonzero Δ. Figure 7 shows the violation versus N for the optimal choices of angles θ and ϕ, and for the optimal value of $\Delta = N - 1$. The violation is maximized by selecting $\Delta = N - 1$, which corresponds to a NOON state at time t_2. Table I shows the values, including the optimal angles, for the case $N = 11$. For $N = 15$, Fig. 7 shows the violation versus Δ.

2. Evaluation of the disturbance inequality

We now outline the calculation of the disturbance inequality. To evaluate $\langle S_3|\hat{M},\sigma\rangle$ we calculate the expectation of S_3 given that a projective (NCP or INR) measurement is made at time t_2, with the state preparation at time t_1 as above for the macroscopic Hong-Ou-Mandel effect. Specifically

$$\begin{aligned}\langle S_3|\hat{M},\sigma\rangle &= \frac{P_+}{P_+ + P_-}\langle S_3\rangle_+ + \frac{P_-}{P_+ + P_-}\langle S_3\rangle_- \\ &= \frac{P_+}{P_+ + P_-}\langle S_2 S_3\rangle_+ - \frac{P_-}{P_+ + P_-}\langle S_2 S_3\rangle_-, \quad \text{(C6)}\end{aligned}$$

where $\langle S_3\rangle_\pm$ are the expectation values for the states defined as $|\psi_\pm\rangle$. To evaluate $\langle S_3|\sigma\rangle$, we find the expectation of S_3 without the measurement at time t_2. From the calculations for the Leggett-Garg inequality

$$\langle S_3|\sigma\rangle = \langle\psi_\Delta|S_3|\psi_\Delta\rangle. \quad \text{(C7)}$$

Applying the above results, we obtain that $d_\sigma = 2$ for $N = 3,\ldots,13$ and $\Delta = N - 1$, using the values of the optimal angles. We also evaluate d_σ for $N = 13,11$ and any value of Δ and we have obtained that $d_\sigma = 2$. The results are consistent with a violation of the disturbance equality (2): $d_\sigma \neq 0$.

TABLE I. Maximum values of the violation of the Leggett-Garg inequalities on optimizing the choice of angles θ and ϕ, for fixed Δ and N.

Δ	N	θ_{opt}	ϕ_{opt}	$LG_{\max}$
1,2	3	0.578973	0.495912	2.33291
1,2	5	0.628767	0.33428	2.11778
1,2	7	0.655977	0.254457	1.9855
1,2	9	0.673675	0.206237	1.89226
1,2	11	0.68629	0.17377	1.82165
1,2	13	0.695819	0.150344	1.76568
3,4	5	0.619339	0.475729	2.67167
3,4	7	0.649188	0.356205	2.51489
3,4	9	0.667305	0.287775	2.39912
3,4	11	0.680023	0.24249	2.30743
3,4	13	0.689619	0.210043	2.23205
5, 6	7	0.64078	0.465008	2.83173
5, 6	9	0.662639	0.36856	2.73091
5, 6	11	0.676442	0.3087	2.6466
5, 6	13	0.686464	0.266797	2.57372
7, 8	9	0.654105	0.458346	2.91181
7, 8	11	0.671783	0.376633	2.84982
7, 8	13	0.683173	0.323265	2.79288
9, 10	11	0.663216	0.45379	2.95311
9, 10	13	0.678323	0.382401	2.91581

APPENDIX D: NOON STATE AT TIME t_2 IN A LINEAR INTERFEROMETER WITH PHASE SHIFT

We consider where a NOON state is created at time t_2, either by dynamical evolution or by using conditional methods as described above. The NOON state with spatially separated modes enables an INR result measurement $\hat{M}$ at time t_2. In Fig. 3(c) we give results for the scheme where, after the measurement at time t_2, the system passes through the linear interferometer modeled by a phase shift ϕ followed by a 50/50 beam splitter. The transformations differ from the linear interferometer described above, which is based on a PBS.

At time t_2 we suppose therefore that the state has evolved to a NOON state given by

$$|\psi(t_2)\rangle = \alpha|N\rangle_c|0\rangle_d + \beta|0\rangle_c|N\rangle_d, \quad \text{(D1)}$$

where α and β are normalization coefficients. We take $\alpha = \cos\vartheta$ and $\beta = \sin\vartheta$. We note that the NOON state can in principle be prepared using the conditional approach described in Appendix B and in the main text, in which case ϑ is determined by the beam splitter angle θ. We also comment that phase factors associated with β can change depending on the method of preparation, as seen on comparison with Eq. (4).

If necessary, such phase factors can be manipulated after the initial state preparation using phase shifts. At t_3 the output state is in $\hat{e}$ and $\hat{f}$ modes as given by

$$|\psi(t_3)\rangle = \frac{1}{\sqrt{2^N}}\sum_{m=0}^{N}\frac{\sqrt{N!}}{\sqrt{m!(N-m)!}} \times(\alpha+\beta e^{iN\phi}(-1)^{N-m})|m\rangle_e|N-m\rangle_f. \quad \text{(D2)}$$

The probability of detecting m photons at mode e and $N-m$ photons at d is

$$P_{m,N-m} = \frac{1}{2^N}\binom{N}{m}[1+2\alpha\beta(-1)^{(N-m)}\cos(N\phi)]. \quad \text{(D3)}$$

We obtain

$$\langle S_1S_2\rangle = \alpha^2-\beta^2 = \cos 2\vartheta,$$
$$\langle S_1S_3\rangle = \sum_{m=0}^{N}\text{sgn}(2m-N)P_{m,N-m}. \quad \text{(D4)}$$

For even N, $\langle S_1S_3\rangle = 0$. Noting that

$$\sum_{m=0}^{N}\text{sgn}(2m-N)\frac{1}{2^N}\binom{N}{m}(-1)^{N-m} = X_N, \quad \text{(D5)}$$

where

$$X_N = \frac{(-1)^{(N-1)/2}\Gamma(N/2)}{\sqrt{\pi}\Gamma((N+1)/2)}$$

we can simplify the correlation to (since $\alpha\beta = \frac{1}{2}\sin 2\vartheta$)

$$\langle S_1S_3\rangle = X_N\sin 2\vartheta\cos N\phi. \quad \text{(D6)}$$

The final correlation is obtained by evaluating the weighted average where $|N\rangle|0\rangle$ and $|0\rangle|N\rangle$ are taken to be the initial state. This is based on the prediction for a nonclumsy projective measurement that collapses the state at time t_2, to either $|N\rangle|0\rangle$ or $|0\rangle|N\rangle$. Thus

$$\langle S_2S_3\rangle = \alpha^2\sum_{m=0}^{N}\text{sgn}(2m-N)|h^{(N)}|^2 -\beta^2\sum_{m=0}^{N}\text{sgn}(2m-N)|h^{(0)}|^2, \quad \text{(D7)}$$

where

$$h^{(N)} = \frac{1}{\sqrt{2^N}}\sqrt{\frac{N!}{m!(N-m)!}}.$$
$$h^{(0)} = \frac{1}{\sqrt{2^N}}\sqrt{\frac{N!}{m!(N-m)!}}e^{iN\phi}(-1)^{N-m}. \quad \text{(D8)}$$

We find that for all values of N, $\langle S_2S_3\rangle = 0$. For example, for $N=3$,

$$|3\rangle|0\rangle \to \frac{1}{\sqrt{8}}(|0\rangle|3\rangle+\sqrt{3}|1\rangle|2\rangle+\sqrt{3}|2\rangle|1\rangle+|3\rangle|0\rangle),$$
$$|0\rangle|3\rangle \to \frac{e^{i3\varphi}}{\sqrt{8}}(-|0\rangle|3\rangle+\sqrt{3}|1\rangle|2\rangle-\sqrt{3}|2\rangle|1\rangle+|3\rangle|0\rangle).$$

TABLE II. Maximum values of the violation of the Leggett-Garg inequalities on optimizing the choice of angles ϑ and ϕ.

N	LG_{max}	ϑ_{opt}	ϕ_{opt}
3	1.11803	−0.231824	$\pi/3$
5	1.068	0.179385	$\pi/5$
7	1.04769	−0.151442	$\pi/7$
9	1.03671	0.1333456	$\pi/9$
11	1.02984	−0.120649	$\pi/11$
13	1.02513	0.110936	$\pi/13$
15	1.0217	−0.103244	$\pi/15$
19	1.01705	−0.0916934	$\pi/19$
21	1.0154	0.0872034	$\pi/21$
51	1.00628	−0.0559035	$\pi/51$
101	1.00316	0.0397109	$\pi/101$

Hence

$$\langle S_2S_3\rangle = \frac{\alpha^2}{8}(1+3-3-1)+\frac{\beta^2}{8}(1+3-3+1) = 0.$$

For N even, there is no violation of the Leggett-Garg inequality (1) since $\langle S_2S_3\rangle = 0$ and $\langle S_1S_3\rangle = 0$. Thus the Leggett-Garg inequality for even N reduces to $LG = \langle S_1S_2\rangle = \cos 2\vartheta < 1$. For odd N, the Leggett-Garg correlation is

$$LG = \cos 2\vartheta - X_N\sin 2\vartheta\cos N\phi. \quad \text{(D9)}$$

Here, it is possible to obtain violations of the Leggett-Garg inequality. The angles ϑ_{opt} and ϕ_{opt} that maximize the value of LG are

$$\vartheta_{\text{opt}} = \tfrac{1}{2}\arctan[X_N],$$
$$\phi_{\text{opt}} = \pi/N. \quad \text{(D10)}$$

Substituting this into the expressions for $\langle S_1S_2\rangle$ and $\langle S_1S_3\rangle$, we obtain for the maximum value

$$LG = \sqrt{1+X_N^2}. \quad \text{(D11)}$$

Table II indicates the maximum Leggett-Garg violation and the optimal values of ϕ and ϑ. The maximum violation is plotted in Fig. 3(c) and in Fig. 8, in this case for N up to 19.

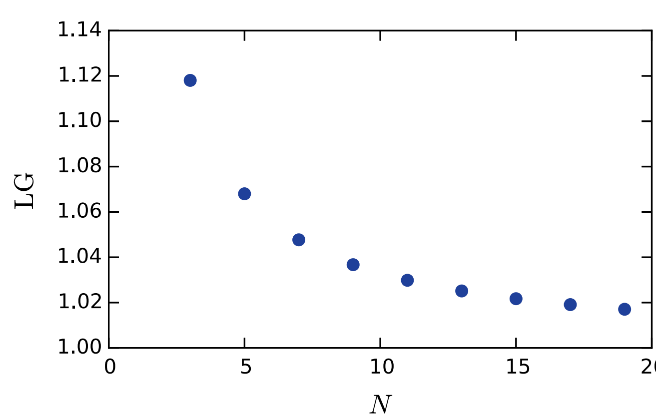

FIG. 8. Violation of the Leggett-Garg inequality up to $N = 19$, for the optimal values of ϑ and ϕ as given in Table II.

TABLE III. The panel on the left gives the maximum violation of the Leggett-Garg inequalities where ϑ is optimized at ϑ_{opt} for the fixed angle $\phi = \pi/4$. The panel on the right gives the maximum violation of the Leggett-Garg inequality where the angle ϑ is optimized at ϑ_{opt}, given the constraint $\phi = \vartheta$.

N	$LG_{\max}$	ϑ_{opt}	N	$LG_{\max}$	ϑ_{opt}
3	1.06066	−0.169918	3	1.08875	0.159386
5	1.03456	0.1296	5	1.0457	−0.107283
7	1.02412	0.108738	7	1.02943	0.0817553
9	1.01852	−0.0954964	9	1.02113	−0.0663958
11	1.01503	−0.0861447	11	1.01618	0.0560665
13	1.01264	0.0790904	13	1.01295	−0.0486131
15	1.01091	0.0735252	15	1.01068	0.0429661
19	1.00856	−0.0652016	19	1.00776	0.0349518
21	1.00773	0.0619757	21	1.00877	0.139267
51	1.00315	−0.0396122	51	1.00622	−0.0610179
101	1.00158	−18.8214	101	1.00302	0.031722

It is also possible to get violations of the Leggett-Garg inequality for fixed choice of angle ϕ. Here we select $\phi = \pi/4$ and find the optimal choice for ϑ is given by

$$\vartheta_{\text{opt}} = -\frac{1}{2}\arctan\left[X_N \cos\left(\frac{\pi N}{4}\right)\right]. \tag{D12}$$

With these values we get the maximum violation

$$LG = \sqrt{1 + \frac{X_N^2}{2}}. \tag{D13}$$

The corresponding values are given in Table III. We also consider the case where $\vartheta = \phi$. Here we obtain violations of the Leggett-Garg inequality for a suitable choice of ϕ as given in Table III. Figure 3(c) gives a summary of the violations of the Leggett-Garg inequality that are possible.

[1] E. Schrödinger, Naturwiss. **23**, 807 (1935).
[2] A. J. Leggett and A. Garg, Phys. Rev. Lett. **54**, 857 (1985).
[3] A. N. Jordan, A. N. Korotkov, and M. Buttiker, Phys. Rev. Lett. **97**, 026805 (2006).
[4] G. C. Knee, K. Kakuyanagi, M.-C. Yeh, Y. Matsuzaki, H. Toida, H. Yamaguchi, S. Saito, A. J. Leggett, and W. J. Munro, Nat. Commun. **7**, 13253 (2016).
[5] C.-M. Li, N. Lambert, Y.-N. Chen, G.-Y. Chen, and F. Nori, Sci. Rep. **2**, 885 (2012); R. E. George, L. M. Robledo, O. J. E. Maroney, M. S. Blok, H. Bernien, M. L. Markham, D. J. Twitchen, J. J. L. Morton, G. A. D. Briggs, and R. Hanson, Proc. Natl. Acad. Sci. USA **110**, 3777 (2013); J. Kofler and C. Brukner, Phys. Rev. A **87**, 052115 (2013); L. Clemente and J. Kofler, *ibid.* **91**, 062103 (2015); Phys. Rev. Lett. **116**, 150401 (2016); K. Wang, G. C. Knee, X. Zhan, Z. Bian, J. Li, and P. Xue, Phys. Rev. A **95**, 032122 (2017).
[6] Emary, N. Lambert, and F. Nori, Rep. Prog. Phys. **77**, 016001 (2014).
[7] A. Palacios-Laloy, F. Mallet, F. Nguyen, P. Bertet, D. Vion, D. Esteve, and A. N. Korotkov, Nat. Phys. **6**, 442 (2010).
[8] J. Dressel, C. J. Broadbent, J. C. Howell, and A. N. Jordan, Phys. Rev. Lett. **106**, 040402 (2011); J.-S. Xu, C.-F. Li, X.-B. Zou, and G.-C. Guo, Sci. Rep. **1**, 101 (2011); V. Athalye, S. S. Roy, and T. S. Mahesh, Phys. Rev. Lett. **107**, 130402 (2011); A. M. Souza, I. S. Oliveira, and R. S. Sarthour, New J. Phys. **13**, 053023 (2011); G. Waldherr, P. Neumann, S. F. Huelga, F. Jelezko, and J. Wrachtrup, Phys. Rev. Lett. **107**, 090401 (2011); H. Katiyar, A. Shukla, K. R. K. Rao, and T. S. Mahesh, Phys. Rev. A **87**, 052102 (2013); J. A. Formaggio, D. I. Kaiser, M. M. Murskyj, and T. E. Weiss, Phys. Rev. Lett. **117**, 050402 (2016); K. Wang, C. Emary, X. Zhan, Z. Bian, J. Li, and P. Xue, Opt. Exp. **25**, 31462 (2017); Z.-Q. Zhou, S. F. Huelga, C.-F. Li, and G.-C. Guo, Phys. Rev. Lett. **115**, 113002 (2015).
[9] G. C. Knee *et al.*, Nat. Commun. **3**, 606 (2012).
[10] C. Robens, W. Alt, D. Meschede, C. Emary, and A. Alberti, Phys. Rev. X **5**, 011003 (2015).
[11] M. E. Goggin, M. P. Almeida, M. Barbieri, B. P. Lanyon, J. L. O'Brien, A. G. White, and G. J. Pryde, Proc. Natl. Acad. Sci. USA **108**, 1256 (2011).
[12] J. P. Groen, D. Ristè, L. Tornberg, J. Cramer, P. C. de Groot, T. Picot, G. Johansson, and L. DiCarlo, Phys. Rev. Lett. **111**, 090506 (2013).
[13] Y. Suzuki, M. Iinuma, and H. F. Hofmann, New J. Phys. **14**, 103022 (2012).
[14] H. Katiyar, A. Brodutch, D. Lu, and R. Laflamme, New J. Phys. **19**, 023033 (2017).
[15] N. Lambert, K. Debnath, A. F. Kockum, G. C. Knee, and W. J. Munro, and F. Nori, Phys. Rev. A **94**, 012105 (2016).
[16] A. Asadian, C. Brukner, and P. Rabl, Phys. Rev. Lett. **112**, 190402 (2014).
[17] C. Budroni, G. Vitagliano, G. Colangelo, R. J. Sewell, O. Gühne, G. Tóth, and M. W. Mitchell, Phys. Rev. Lett. **115**, 200403 (2015); G. Vitagliano, presentation at Workshop in Temporal Quantum Correlations and Steering, Siegen (unpublished).
[18] Y. Aharonov, D. Z. Albert, and L. Vaidman, Phys. Rev. Lett. **60**, 1351 (1988); N. S. Williams and A. N. Jordan, *ibid.* **100**, 026804 (2008).
[19] G. J. Pryde, J. L. O' Brien, A. G. White, T. C. Ralph, and H. M. Wiseman, Phys. Rev. Lett. **94**, 220405 (2005).
[20] J. Dressel, M. Malik, F. M. Miatto, A. N. Jordan, and R. W. Boyd, Rev. Mod. Phys. **86**, 307 (2014).
[21] J. Dressel and A. N. Korotkov, Phys. Rev. A **89**, 012125 (2014); T. C. White *et al.*, NPJ Quantum Inf. **2**, 15022 (2016); B. L. Higgins, M. S. Palsson, G. Y. Xiang, H. M. Wiseman, and G. J. Pryde, Phys. Rev. A **91**, 012113 (2015).
[22] L. Rosales-Zárate, B. Opanchuk, and M. D. Reid, Phys. Rev. A **97**, 032123 (2018).
[23] A. Leggett, Found. Phys. **18**, 939 (1988); M. Wilde and A. Mizel, *ibid.* **42**, 256 (2011).
[24] G. C. Ghirardi, A. Rimini, and T. Weber, Phys. Rev. D **34**, 470 (1986); L. Diósi, Phys. Lett. A **120**, 377 (1987); R. Penrose, Gen. Relativ. Gravit. **28**, 581 (1996).

[25] J. P. Dowling, Contemp. Phys. **49**, 125 (2008); I. Afek, O. Ambar, and Y. Silberberg, Science **328**, 879 (2010); M. W. Mitchell, J. S. Lundeen, and A. M. Steinberg, Nature (London) **429**, 161 (2004); P. Walther, J.-W. Pan, M. Aspelmeyer, R. Ursin, S. Gasparoni, and A. Zeilinger, *ibid.* **429**, 158 (2004).

[26] S. Slussarenko, M. M. Weston, H. M. Chrzanowski, L. K. Shalm, V. B. Verma, S. W. Nam, and G. J. Pryde, Nat. Photonics **11**, 700 (2017).

[27] R. Lopes, A. Imanaliev, A. Aspect, M. Cheneau, D. Boiron, and C. I. Westbrook, Nature (London) **520**, 66 (2015); R. J. Lewis-Swan and K. V. Kheruntsyan, Nat. Commun. **5**, 3752 (2014).

[28] J. S. Bell, Physics **1**, 195 (1964).

[29] M. Albiez, R. Gati, J. Fölling, S. Hunsmann, M. Cristiani, and M. K. Oberthaler, Phys. Rev. Lett. **95**, 010402 (2005).

[30] G. J. Milburn, J. Corney, E. M. Wright, and D. F. Walls, Phys. Rev. A **55**, 4318 (1997); J. Dunningham and K. Burnett, J. Mod. Opt. **48**, 1837 (2001); D. Gordon and C. M. Savage, Phys. Rev. A **59**, 4623 (1999); T. J. Haigh, A. J. Ferris, and M. K. Olsen, Opt. Commun. **283**, 3540 (2010).

[31] J. I. Cirac, M. Lewenstein, K. Mølmer, and P. Zoller, Phys. Rev. A **57**, 1208 (1998).

[32] Y. Zhou, H. Zhai, R. Lu, Z. Xu, and L. Chang, Phys. Rev. A **67**, 043606 (2003).

[33] L. D. Carr, D. R. Dounas-Frazer, and M. A. Garcia-March, Europhys. Lett. **90**, 10005 (2010); D. R. Dounas-Frazer, A. M. Hermundstad, and L. D. Carr, Phys. Rev. Lett. **99**, 200402 (2007).

[34] B. Opanchuk, L. Rosales-Zárate, R. Y. Teh, and M. D. Reid, Phys. Rev. A **94**, 062125 (2016); L. Rosales-Zárate, B. Opanchuk, Q. Y. He, and M. D. Reid, arXiv:1612.05726 [quant-ph].

[35] K. Pawłowski, M. Fadel, P. Treutlein, Y. Castin, and A. Sinatra, Phys. Rev. A **95**, 063609 (2017).

[36] J. Estève, C. Gross, A. Weller, S. Giovanazzi, and M. K. Oberthaler, Nature (London) **455**, 1216 (2008).

[37] C. Gross, T. Zibold, E. Nicklas, J. Estève, and M. K. Oberthaler, Nature (London) **464**, 1165 (2010).

[38] M. F. Riedel, P. Böhi, Y. Li, T. W. Hänsch, A. Sinatra, and P. Treutlein, Nature (London) **464**, 1170 (2010).

[39] N. Bar-Gill, C. Gross, I. Mazets, M. Oberthaler, and G. Kurizki, Phys. Rev. Lett. **106**, 120404 (2011); Q. Y. He, M. D. Reid, T. G. Vaughan, C. Gross, M. Oberthaler, and P. D. Drummond, *ibid.* **106**, 120405 (2011).

[40] K. Lange, J. Peise, B. Lücke, I. Kruse, G. Vitagliano, I. Apellaniz, M. Kleinmann, G. Toth, and C. Klempt, arXiv:1708.02480.

[41] P. Kunkel, M. Prüfer, H. Strobel, D. Linnemann, A. Frölian, T. Gasenzer, M. Gärttner, and M. K. Oberthaler, arXiv:1708.02407; M. Fadel, T. Zibold, B. Décamps, and P. Treutlein, arXiv:1708.02534.

[42] Q. Y. He, P. D. Drummond, M. K. Olsen, and M. D. Reid, Phys. Rev. A **86**, 023626 (2012); B. Opanchuk, Q. Y. He, M. D. Reid, and P. D. Drummond, *ibid.* **86**, 023625 (2012).

[43] D. Alcala, J. Glick, and L. Carr, Phys. Rev. Lett. **118**, 210403 (2017).

[44] M. J. Steel and M. J. Collett, Phys. Rev. A **57**, 2920 (1998); H. J. Lipkin, N. Meshkov, and A. J. Glick, Nucl. Phys. **62**, 188 (1965).

[45] K. K. Likharev, Rev. Mod. Phys. **51**, 101 (1979); C. Wang *et al.*, Science **352**, 1087 (2016); S. Zeytinoğlu, M. Pechal, S. Berger, A. A. Abdumalikov, Jr., A. Wallraff, and S. Filipp, Phys. Rev. A **91**, 043846 (2015); C. Eichler, Y. Salathe, J. Mlynek, S. Schmidt, and A. Wallraff, Phys. Rev. Lett. **113**, 110502 (2014).

[46] S. Backhaus, S. Pereverzev, R. W. Simmonds, A. Loshak, J. C. Davis, and R. E. Packard, Nature (London) **392**, 687 (1998).

[47] M. Abbarchi *et al.*, Nat. Phys. **9**, 275 (2013).

[48] D. Ananikian and T. Bergeman, Phys. Rev. A **73**, 013604 (2006).

[49] M. Egorov, R. P. Anderson, V. Ivannikov, B. Opanchuk, P. Drummond, B. V. Hall, and A. I. Sidorov, Phys. Rev. A **84**, 021605(R) (2011).

[50] O. J. E. Maroney and C. G. Timpson, arXiv:1412.6139v1.

[51] E. O. Ilo-Okeke and T. Byrnes, Phys. Rev. Lett. **112**, 233602 (2014); J. J. Hope and J. D. Close, *ibid.* **93**, 180402 (2004).

[52] A. Chantasri, J. Dressel, and A. N. Jordan, Phys. Rev. A **88**, 042110 (2013); J. F. Ralph, K. Jacobs, and M. J. Everitt, *ibid.* **95**, 012135 (2017); J. K. Eastman, J. Hope, and A. R. Carvalho, Sci. Rep. **7**, 44684 (2017).

[53] M. Stobińska, F. Töppel, P. Sekatski, A. Buraczewski, M. Żukowski, M. V. Chekhova, G. Leuchs, and N. Gisin, Phys. Rev. A **86**, 063823 (2012); T. Sh. Iskhakov, K. Yu Spasibko, M. V. Chekhova, and G. Leuchs, New J. Phys. **15**, 093036 (2013); K. Yu Spasibko, F. Töppel, T. Sh Iskhakov, M. Stobińska, M. V. Chekhova, and G. Leuchs, *ibid.* **16**, 013025 (2014); G. J. Pryde and A. G. White, Phys. Rev. A **68**, 052315 (2003); A. E. B. Nielsen and K. Mølmer, *ibid.* **75**, 063803 (2007).

[54] E. G. Cavalcanti and M. D. Reid, Phys. Rev. Lett. **97**, 170405 (2006); Phys. Rev. A **77**, 062108 (2008); C. Marquardt, U. L. Andersen, G. Leuchs, Y. Takeno, M. Yukawa, H. Yonezawa, and A. Furusawa, *ibid.* **76**, 030101R (2007).

[55] M. D. Reid, Phys. Rev. A **97**, 042113 (2018).

[56] R. I. Khakimov, B. M. Henson, D. K. Shin, S. S. Hodgman, R. G. Dall, K. G. H. Baldwin, and A. G. Truscott, Nature (London) **540**, 100 (2016); C. Gross, H. Strobel, E. Nicklas, T. Zibold, N. Bar-Gill, G. Kurizki, and M. K. Oberthaler, *ibid.* **480**, 219 (2011).

[57] T. Kovachy, P. Asenbaum, C. Overstreet, C. A. Donnelly, S. M. Dickerson, A. Sugarbaker, J. M. Hogan, and M. A. Kasevich, Nature (London) **528**, 530 (2015).

[58] K. S. Hardman, P. B. Wigley, P. J. Everitt, P. Manju, C. C. N. Kuhn, and N. P. Robins, Opt. Lett. **41**, 2505 (2016).